NASA CONTRACTOR REPORT

FATIGUE BEHAVIOR OF A FUSION WELDED Ti-8Al-1Mo-1V SIMULATED WING STRUCTURE UNDER THE ENVIRONMENT OF A SUPERSONIC TRANSPORT

by John J. Peterson

Prepared by
LTV AEROSPACE CORPORATION
Dallas, Texas
for Langley Research Center

NATIONAL AERONAUTICS AND SPACE ADMINISTRATION • WASHINGTON, D. C. • SEPTEMBER 1967

NASA CR-881

FATIGUE BEHAVIOR OF A FUSION WELDED Ti-8Al-1Mo-1V SIMULATED WING STRUCTURE UNDER THE ENVIRONMENT OF A SUPERSONIC TRANSPORT

By John J. Peterson

Prepared under Contract No. NAS 1-5495 by
LTV AEROSPACE CORPORATION
Dallas, Texas

for Langley Research Center

NATIONAL AERONAUTICS AND SPACE ADMINISTRATION

For sale by the Clearinghouse for Federal Scientific and Technical Information
Springfield, Virginia 22151 – CFSTI price $3.00

FATIGUE BEHAVIOR OF A FUSION WELDED Ti-8Al-1Mo-1V SIMULATED WING STRUCTURE UNDER THE ENVIRONMENT OF A SUPERSONIC TRANSPORT

By John J. Peterson
LTV Aerospace Corporation
Vought Aeronautics Division

SUMMARY

A test program was conducted to evaluate the fatigue behavior of a fusion welded structural assembly. This work was done to supplement information which was generated earlier by testing riveted and spot-welded structures.

These present tests were performed on box-beams having tension covers featuring typical skin-stringer welded structures. The material used was Ti-8Al-1Mo-1V in the duplex annealed condition. Both constant amplitude and spectrum fatigue tests were conducted. Tests were performed at room temperature and 550°F. Spectrum tests were conducted under conditions which simulated the environment of the SST. Four specimens were fabricated and tested.

INTRODUCTION

The SST represents a significant advance in the state-of-the-art of aircraft design and operation and, as such, will create problems which are new and unique. Simple economics dictate the need for an airframe having both a high level of structural efficiency and a long service life. In order to attain these goals major emphasis must be placed on design for fatigue. In an effort to supplement the relatively meager store of fatigue information for materials and structures operating under the environment of the SST, the National Aeronautics and Space Administration has been actively engaged in sponsoring fatigue research programs. See, for example, references (1) and (2).

The program which is reported herein is a further extension of this effort and was sponsored by the National Aeronautics and Space Administration under Contract NAS1-5495.

During the program reported earlier in reference (1) a series of box beam tests were conducted on typical sheet-stringer panels considered representative of wing skin structures suited for use on the SST. These panels were fabricated by "conventional" means, i.e. spotwelding and riveting were employed as the basic joining media.

From the standpoint of design efficiency and/or overall cost effectiveness the fusion welded structure has much to offer. Among the advantages to be gained with welded structures are the elimination of large numbers of fasteners and their attendant fatigue problems, and improved efficiency in effecting load transfer. However, a fundamental disadvantage to be expected in using an all welded structure stems from the lack of inherent crack stopping, or fail safe, capabilities.

In order to provide designers with information to aid in the final selection of structural arrangements, the test program described in this report was conducted. Four fusion welded panels were fabricated and tested under the same conditions as those used in testing the spotwelded and riveted panels reported in reference (1). Within the limits of the processes utilized, all panels also had the same geometries. Comparisons were also made between the test results contained in this report and those for both spotwelded and riveted specimens reported in reference (1).

SYMBOLS

C.A.	constant amplitude
f	frequency of occurrence of flight load
GAG	ground-air-ground cycle, variation in load factor associated with the transfer of load from the landing gear to the wing and back to the landing gear.
G.L.	test specimen gage length - inches
K_t	theoretical stress concentration factor
l_c	crack length - inches
L.F.	airplane load factor
R	stress ratio, the ratio of the minimum to the maximum stress during a load cycle
S_{tu}	ultimate tensile stress
S_{alt}	alternating stress in a fatigue cycle

S_{1g_D} stress level at take-off design gross weight - one g

S_{mean} the algebraic mean of the maximum and minimum stress in one cycle: $S_{mean} = (S_{max} + S_{min})/2$

S_{max} the highest algebraic value of stress in the stress cycle with tensile stresses positive

S_{min} the lowest algebraic value of stress in the stress cycle with tensile stresses positive

S_T thermal stress component, $0.65 \times S_{1g_D}$

W* ratio of instantaneous airplane weight to take-off gross weight

Θ a non-dimensional parameter which expresses the ratio of the alternating stress component of a cycle to S_{1g_D}

SPECIMEN DESIGN

General.- A box-beam 120 inches long, 22.50 inches wide and 8.0 inches deep (which was designed for use as a test vehicle in the program described in reference (1)) was also utilized during this investigation. This box-beam consisted of two separate assemblies:(1) a tension cover simulating typical sheet stringer construction, which was used as a test specimen, and (2) the balance of the box-beam structure consisting of a compression cover, internal and external shear webs and bulkheads to stabilize the test specimen. The beams were designed to impart constant bending moments to the test specimens. Hydraulic actuators were employed to apply the loads to the test structure through axles which were located on the neutral axis of the box-beam assembly. This arrangement effectively minimized the possibility of applying eccentric moments on the test article. A sketch showing the general arrangement of the box-beam and test set up is shown in Figure 1.

Test Skins.- A total of four tension skin test specimens were fabricated from duplex annealed Ti-8Al-1Mo-1V titanium alloy for use during this program. In order that the results obtained during this investigation might be as meaningful as possible, the welded specimen geometries duplicated, as nearly as possible, the geometries of the panels tested earlier in the program described in reference (1).

The specimens were sheet-stringer panels measuring 120 inches by 22.50 inches. The panels contain five length-wise stiffeners as shown in the sketch of Figure 2. Figure 3 is a photograph showing internal details of the test section of the panel. As seen in this photograph, the

panel contains typical stress raisers in the form of a transverse splice at the panel centerline, a small reinforced cut-out, and a large structural door. Also visible in this photograph are the typical chem-milled reinforcements which duplicated the local material build-up which was accomplished by the use of spotwelded and/or riveted doublers on the panels reported in reference (1). General constructional details in the vicinity of these stress raisers are shown in the drawings of Figures 4, 5, and 6.

The test panels were fabricated through the use of fusion welding techniques as described in Appendix A to this report.

Box Beam Fixtures.- The reusable box-beam fixtures which were described in reference (1), were undamaged and were considered suitable for the test program described herein. A photograph which shows the internal arrangement of this fixture is shown in Figure 7.

TEST FIXTURES AND EQUIPMENT

Test fixtures designed to impose constant bending moments over the length of the test section, as shown in the sketch of Figure 1, were used during this program. Where necessary, elevated temperatures were attained through the use of radiant lamp furnaces which were large enough to enclose the entire box beam assembly, as shown in Figure 9 of reference (1).

Test loads were applied to the specimen by a pair of 50,000 pound capacity servo controlled hydraulic actuators. The necessary commands to these actuators were supplied by a computer controlled electronic programmer. This system consists of three basic elements; the computer and core memory, the ramp generation units and the servo-valve controllers. Eight independent load channels may be controlled by this system.

The computer has a core capacity of 1028 locations which may be addressed sequentially, randomly or, by a computed go-to instruction.

Prepunched information describing the controlled load channel or channels, the load rate and the load level is entered into the computer information register from a tape reader. This information, when called for, is then used to drive the ramp generators to the desired output levels. A calibrated load ring, in series with the hydraulic actuator, generates a feedback signal which is compared to the original command signal for the purpose of balancing the system. Corrective loads are applied until the difference between the two signals is reduced to zero. In the event that the signal differences are larger than a preset value, the system then shuts down.

Since a hydraulic system of this type is not capable of an instantaneous load reduction in the event of a specimen failure, additional

safety features are built into the test fixture to protect the reusable box-beam in the event of a catastrophic failure of the test specimen. These consisted of physical stops to effectively prevent excessive deflections during the period of time when the load was dropping off.

MATERIALS

The original program plans were based on the use of triplex annealed Ti-8Al-1Mo-1V material in order to facilitate comparison of the test results with those published earlier in reference (1). It proved, however, impossible to procure the material in the desired heat treated condition and a change to duplex annealed material was made. It was concluded that, when compared on a non-dimensional basis, the fatigue lives of the duplex and triplex annealed Ti-8Al-1Mo-1V would be similar, see Appendix B. The material procured for this program had the following chemical composition, processing history and mechanical properties:

Chemical Composition

Element	Percent t = 0.050	t = 0.100	t = 0.150
Carbon	0.020	0.020	0.020
Nitrogen	0.006	0.006	0.007
Iron	0.080	0.080	0.080
Aluminum	8.10	8.10	7.80
Vanadium	1.10	1.10	1.10
Modybdenum	1.00	1.00	1.10
Oxygen	0.082	0.078	0.106
Hydrogen	0.0054	0.0040	0.0039

Processing History

1. Anneal at 1450°F for 8 hours, furnace cool; reheat at 1450°F for 15 minutes and air cool.

2. Final finish by pickle and grind.

Mechanical Properties Reported by Producer - (Londitudinal Grain)

	t = 0.050	t = 0.100	t = 0.150
S_{tu} *	145 800 149 300	148 600 146 000	144 200 147 500
S_{ty} *	136 800 142 500	139 000 140 600	134 800 137 400
Elongation, % *	12 14	14 16	12 16

* Maximum and Minimum values from 16 tests of each thickness

Mechanical property tests were conducted on "as received" material as well as on welded samples prior to actual specimen fabrication, tests were conducted at both room temperature and 550°F. The results of these tests are shown in Table I.

TEST CONDITIONS

Spectrum.- The loading schedule developed for use during the program of reference (1) was used for spectrum testing during this investigation. Contained in this spectrum are GAG loads, gust and maneuver loads, loads occurring during check flights, and loads due to thermal stresses. Although the basic loading schedule contains loads for climb, cruise and descent, the test schedule contains only climb and cruise loads since descent loads are below the material endurance limit.

The basic spectrum, which is representative of approximately 30 000 hours of flying time, is shown in Table II. The spectrum contains loads for 12 500 flights (12 000 operational and 500 check flights).

The mean stresses applied to the specimen during testing were varied to reflect changes in the vehicle gross weight during a flight. The relative value of this mean (or 1g) stress level is defined by W* which is the ratio of instantaneous gross weight to the take-off gross weight, S_{1g_D}. Since S_{1g_D} = 25 000 psi, the nominal mean stress at any time is $(W^*)(25\ 000)$.

During this program the following values of W* were used:

a. Take-off and climb, W* = 1.0

b. Cruise, W* = 0.75

c. Check flights, W* = 0.70

The alternating stress components are defined in terms of θ which is also related to S_{1g_D}. The maximum stress in any cycle is:

$$S_{max} = S_{mean} + S_{alt} = (S_{1g_D})(W^* + \theta)$$ for take-off, climb and check flight loads.

The test fixture described earlier was designed to keep applied thermal stresses to a minimum. In order to simulate thermal stresses, which might reasonably develop during the course of a flight, the mean stress used during the cruise portion of the flight was increased by an amount equal to (0.65) (S_{1g_D}). The maximum stress during cruise may then be defined as:

$$S_{max} = (S_{1g_D})(W^* + \Theta + 0.65) = (S_{1g_D})(1.40 + \Theta)$$

Practical limitations in heating and cooling made true flight by flight simulation of loads impossible. Therefore a block test was conducted with each block containing two percent of the total spectrum.

Since the probability of gust and maneuver loads occurring during the heated portion of the climb profile is small, all GAG, climb and check flight loads were applied to the specimen at ambient temperature. All cruise loads were applied at a temperature of 550°F.

Those loads which were imposed on the specimen at ambient temperature were applied on a flight by flight basis for best simulation of the effects of the ground-air-ground cycle on fatigue life. The cruise loads were applied in the form of a random group which contained all of the loads for the previously imposed 240 operational flights. Loads occurring with a frequency of less than once per block were inserted in randomly selected blocks during the test.

A breakdown of the manner in which spectrum loads were applied to the specimens is shown in Tables II, III and IV of reference (1), as described below.

Table II lists the number of load cycles applied to the specimens on a flight by flight basis including check flight loads. These loads were applied at ambient temperature.

TableIII presents the loads applied during the heated (cruise) portion of each block.

Those loads whose frequency of occurrence was less than once per block were applied in randomly selected blocks as shown in Table IV.

Constant Amplitude.- Constant amplitude tests were conducted to establish the basic fatigue characteristics of the test specimens and to be used for correlation with available simple element fatigue data.

One specimen was tested under GAG loads (S_{max} = 25 ksi, S_{min} =-12.5 ksi) since this load was felt to be the largest single contributor to overall fatigue damage. This test was performed at room temperature.

A second specimen was tested to observe the effects of elevated temperatures on fatigue behavior. This test was conducted at 550°F under the cruise load condition having the highest frequency of occurrence (S_{max} = 41.25 ksi, S_{min} = 28.75 ksi).

TEST PLAN

Four fusion welded specimens were fabricated and tested during the course of this program. Tests were performed as follows:

Specimen No. 1	Constant Amplitude, GAG Loads, RT, S_{max} = +25 ksi, S_{min} = -12.5 ksi
Specimen No. 2	Constant Amplitude, Cruise Loads, 550°F, S_{mean} = 35 ksi, S_{alt} = +6.25 ksi
Specimen No's 3 & 4	Spectrum Tests, S_{lgD} = 25 ksi, RT and 550°F

Proof loads were applied to the first test specimen to obtain strain information from strain gages and photoelastic coatings.

PROOF LOAD TEST

Prior to initiation of fatigue tests specimen number 1 was extensively instrumented with both strain gages and a photoelastic coating, which covered the entire test section, to aid in the determination of strain distributions. Proof loads were applied to the specimen in 2500 pound increments up to a maximum load of 20 000 pounds, which is the theoretical load required to produce a nominal skin stress of 25 000 psi in the test section. At each load level all strain gages were read and the photoelastic coating was carefully observed for signs of abnormal specimen behavior. Color photographs were taken over the entire test section at loads of 10 000 at 15 000 and 20 000 pounds as a permanent record of surface strain distributions. In addition a set of normal incidence readings were obtained directly from the plastic at the 20 000 pound load level. Additional observations made at this time established the fact that the direction of the maximum principal stresses was within 3° of the longitudinal axis of the specimen over the length of the test section.

Strain gage readings obtained during the proof load test are presented in Table VI. All data points are recorded in accordance with the sign convention illustrated in Figure 2. Figure 8 is a composite photograph showing isochromatics observed in the test section at an applied load of 15 000 pounds and Figure 9 presents stress contours at various sections of the test specimen at a load of 20,000 pounds.

REPEATED LOAD TESTS

General.- For the small specimens which are generally used to generate fatigue data on structural materials it is difficult, and often impossible,

to determine the number of load cycles occurring between the initiation of a crack and final rupture of the specimen. For this reason these data are generally plotted as stress vs cycles to failure. However, in the case of a large, complex, specimen the initiation and propagation of fatigue cracks may be easily monitored. Under normal circumstances there are many cycles of applied load between crack initiation and the ultimate length of several inches. Although tests were continued, in some cases, to a point where one or more long cracks were present in the specimen, the structure is considered unsuited for further use when at least one crack has reached a length of 0.50 inch. Crack initiation is defined as the point when a crack has reached a length of 0.03 inch, which is the smallest crack which can be readily detected during normal visual inspections.

Summary of Results.- A brief summary of the tests conducted on fusion welded, spot welded and riveted specimens is shown in Table VII.

Description of Failures.- Unlike the cracks observed during the program reported in reference (1), those fatigue cracks observed during this investigation were non-preferential in location. All cracks, however, initiated in welded areas. In addition, with the exception of crack number 1, specimen number 1, all cracks initiated in weld metal which was oriented parallel to the direction of applied load. Visual inspection indicated that all cracks initiated in the skin. In most cases the presence of fatigue damage was preceded by a small strained depression in the surface of the panel. Examination of the strained areas using 5x to 10x magnification generally revealed the presence of an extremely small crack at the base of the depression.

Broadly speaking the fatigue cracks observed during this series of tests may be placed in one of two general categories:

a. Small, slow growing cracks which were confined to the weld zone during the duration of the test.

b. Large, fast growing cracks which propagated out of the weld zone soon after detection and continued to grow during the remainder of the test. These cracks also created substructure damage in one or more stiffeners.

A total of 36 identifiable damage sites were observed during these tests; 29 were of the slow growing type and 7 were fast growing.

Figures 10 through 16 are photographs which illustrate typical damaged areas attributable to fast growing fatigue cracks.

Test Specimen Number 1: After proof loading, this specimen was subjected to constant amplitude testing at room temperature under GAG loads (S_{max} = 25 000 psi, S_{min} = -12 500 psi). During a routine inspection, performed after 19 266 load cycles, a large crack, which is shown in the photograph of Figure 17, was detected. The length of this crack was approximately 0.90 inch and it was located on the edge of a repair welded area. Also shown on this photograph is an approximate layout showing the underside of the test skin in this area.

The exact time at which this crack initiated is unknown since the last previously scheduled inspection was performed after completion of 9 114 load cycles at which time the specimen showed no indications of damage.

Since no other damaged areas could be found in this specimen a decision was made to repair weld the damaged area and continue the test thus affording a further opportunity to observe the fatigue performance of an area containing a repair weld, as well as to permit further evaluation of the remainder of the test specimen. Accordingly, the necessary tooling was fabricated and the crack was repaired. A photo showing the repaired area prior to grinding flush is shown in Figure 18.

Testing was resumed at this time and after completion of 21 233 total cycles two additional cracks were detected. These cracks were also in a repair welded area. After 52 877 cycles of load had been applied to the test specimen a total of 11 fatigue cracks had been noted having lengths up to approximately six inches, and the test was discontinued. In addition to the surface cracks described above, one stiffener was severed in two places and cracks had grown into two additional stiffeners. It should be noted at this time that no further damage was observed in the repair welded area shown in Figure 18. A copy of the inspection log for this specimen is shown as Table VII, a sketch showing the location of all cracks is shown in Figure 19, and crack growth data for selected cracks are plotted in Figure 20.

Test Specimen Number 2: This specimen was tested under constant amplitude loading at 550°F with S_{max} = 41 250 psi and S_{min} = 28 750 psi.

After completion of 301 364 load applications the specimen contained no visible indications of fatigue damage and testing was discontinued.

Test Specimen Number 3: Specimen number 3 was tested under spectrum loading conditions with S_{1gD} = 25 000 psi. The first signs of fatigue damage were observed after the completion of 21 blocks of testing (5 250 flights). These fatigue indications were in the form of 3 rather small depressions having lengths from 0.04 to 0.06 inch. The test was continued until the completion of 12 500 flights at which time a total of 11 cracks and/or strain deformed areas had been noted, none of which had attained a length of 0.50 inch. Pertinent data are presented in the inspection log shown as Table VIII and the location of these damaged areas is shown in the sketch of Figure 21. Crack growth data are shown in Figure 22.

Test Specimen Number 4: This specimen was also tested under spectrum loading conditions with S_{1gD} = 25 000 psi. Routine inspections, performed at 250 to 500 flight intervals, revealed no fatigue damage after completion of 2 500 flights. However, an unscheduled inspection, performed during the room temperature portion of spectrum block 11 disclosed the presence of 2 damage sites. The most prominent of these areas appeared to have originated at the edge of the chem-milled recess into which the door was fitted. The visible portion of this crack was approximately 0.25 inch long and, under 5x to 10x magnification, showed little indication of necking as opposed to the behavior in other cracks. A further inspection, amde with the door removed,

showed the crack to have an overall length of 0.50 inch and verified the initial observation with respect to the origin of this crack.

The test was continued until a total of 12 000 flights (48 blocks) had been sustained by the specimen at which time a total of 12 cracks had been observed, and the initial crack had attained a visible length of 3.45 inches. Just prior to the completion of the elevated temperature portion of block 49, a loud noise was heard from the test specimen. After removal of the furnace, an inspection revealed that crack number 1 had grown rapidly to a total visible length of 6.96 inches and the test was stopped. The inspection log for this specimen are shown as Figure 24.

Upon removal of the specimen from the fixture, an internal inspection revealed that the stiffener immediately under the crack was completely severed and that the adjacent stiffener had sustained a crack in the skin attach leg which was approximately 1.25 inches in length. This inspection also revealed the fact that this crack had grown inwards (under the door) an additional distance of 1.50 inches giving this crack a total length of 8.45 inches.

FATIGUE ANALYSIS

Fatigue predictions were made for these specimens for comparison with the test results. The data used for these analyses were:

1. Estimated fatigue life curves for longitudinal fusion welds in duplex annealed Ti-8Al-1Mo-1V as described in Appendix B to this report.

2. S-N data for notched (K_t = 4.0) specimens as presented in reference (3).

3. Longitudinal fusion weld fatigue life curves per reference (2).

Estimated fatigue lives which were derived using these data are as shown in the following table:

Spec. No.	Test Conditions	Predicted Life (Based on Simple Element Test Data)		
		Reference (2)	Reference (3)	Appendix B
1	C.A., GAG loads	10^7 cyc.	9.0×10^4 cyc.	∞
2	C.A., 550°F	∞	5.0×10^5 cyc.	∞
3,4	Spectrum loads	5.6×10^5 flts.	2.9×10^4 cyc.	∞

It can be seen that fatigue life predictions based on the data contained in reference (2) and Appendix B were many times higher than those obtained through the use of reference (3). Although no substantiating data are available at this time, it is felt that weld residual stresses; which are discussed in a later section of this report; contributed significantly to these differences. In addition, the data contained in reference (3) resulted in improved correlation with the observed fatigue lives of the fusion welded specimens at $l_c = 0.50$ inch indicating that the fusion welded specimens tested during this program had an apparent stress concentration factor which was in excess of 4.0.

DISCUSSION

Constant Amplitude Tests.- There was no apparent agreement between the results of the constant amplitude tests conducted during this program with respect to either crack location or relative test life. As noted earlier, the specimen tested under GAG loading contained a total of 11 cracks having lengths up to approximately 6 inches while the specimen tested at 550°F contained no apparent fatigue damage. The fatigue cracks in specimen number 1 were randomly located and did not appear related to either specimen geometry or to the location of any internal defects as determined by X-ray inspection.

The most reasonable estimates of fatigue life for these tests were obtained through the use of the simple element fatigue data contained in reference (3).

Spectrum Tests.- Although both specimens tested under spectrum loading conditions contained a similar number of fatigue damage sites, which were randomly oriented within the test section, the specimens behaved in widely differing manners. Specimen number 3 sustained 12 500 flights of spectrum testing during which time no cracks had reached a length of 0.50 inch. Under the same loading conditions specimen number 4 contained one crack which attained a length of 0.50 inch early in the test (2 750 flights) and, which ultimately precipitated rapid crack growth after 12 250 flights.

As in the case of the constant amplitude tests, the most reasonable predictions of fatigue life were obtained through the use of the notched (K_t = 4.0) fatigue data contained in reference (3).

Fatigue Crack Behavior.- As noted previously, there was no apparent relationship between either the location or the relative order of appearance of fatigue cracks during these tests and, in addition, the number of cracks observed did not appear related to the type of test.

Due to the periodic nature of specimen inspection during the course of a test it was not always possible to determine the specific order in which cracks appeared. However, in all tests, those cracks which ultimately attained the greatest lengths were in the first group of cracks noted during these inspection periods.

For those cracks which attained lengths in excess of 0.50 inch, the overall behavior was similar. Early growth was observed at a relatively uniform rate until a length of approximately 0.25 to 0.50 inch was attained at which time a definite increase in growth rate was noted. This rate then remained relatively constant for the duration of the test.

Residual Stresses.- Typical data on the fatigue behavior of fusion welded Ti-8Al-1Mo-1V (See references (2) and (4) indicate that; for the stress levels used during this program, fatigue lives considerably higher than those observed might reasonably be expected. However, a major obstacle to the accurate prediction of the fatigue life of a welded structure from standard fatigue data is that the complex system of residual stresses which are usually present in a welded structure often do not exist in the simple test specimens. Generally speaking, these residual stresses are a direct result of the restraints imposed on the cooling weld metal by the unheated portions of the adjacent structure. Significant differences in these stresses may often occur even in supposedly identical structures, as a result of slight differences in the rate at which the weld puddle is chilled, clamping pressure, gas flow, etc. Repair welds, which may be made at any time during the history of a welded structure, are another source of residual stresses which must be given consideration.

Stress relief, which would undoubtedly reduce the residual stress magnitude, was not employed during this program in order to insure that these panels might be considered representative of the minimum fatigue performance available from a welded structure.

Although the magnitude of the residual stresses in the welded areas of those panels tested during this program is unknown, it is felt that these stresses were contributory to the reduced fatigue lives observed. The sketch of Figure 25 has been prepared in an effort to furnish some insight into the influence of these stresses. From this sketch it can be seen that a residual tensile stress may alter the fatigue characteristics of a welded structure thus pointing up the need to establish fabrication and/or heat treatment techniques which will minimize residual stresses to the greatest degree possible.

Comparison of Constant Amplitude and Spectrum Tests.- The test results obtained during this investigation were compared by assuming that the experimental and calculated fatigue lives under spectrum and constant amplitude loading conditions would be related in the same manner.

The calculated spectrum life, which was based on the use of the linear cumulative damage theory, and the fatigue life data for simple specimens as reported in reference (3) was multiplied by the ratio of the box beam constant amplitude life to the constant amplitude life of the simple specimens to obtain a corrected life prediction. This predicted life was then compared to the box beam test lives obtained under spectrum loading conditions.

The results of this comparison are presented in Table X where it can be seen that the constant amplitude and spectrum fatigue lives could not be related to one another in a consistent manner.

COMPARISON OF FATIGUE BEHAVIOR BETWEEN SPOTWELDED, RIVETED AND FUSION WELDED TEST SPECIMENS

General.- This section of the report will be devoted to a summary and comparison of the overall fatigue behavior of the riveted and spotwelded specimens tested during the program reported in reference (1) and the behavior of the fusion welded specimens reported herein.

Constant Amplitude Tests.- Although all three panel configurations exhibited fatigue lives which were similar, when based on a crack length of 0.50 inch, the panels jointed by fusion welding were slightly superior in this respect. The number of cracks observed could not be related to test conditions. However, the total number of cracks observed in either the spotwelded or the riveted specimens were approximately five times greater than the number seen in the fusion welded specimens.

A lack of representative fatigue life data for fusion welded structures resulted in overestimated fatigue life predictions when compared to those obtained for spotwelded and riveted assemblies as reported in reference (1).

Spectrum Tests.- Considerable disagreement was seen between the test lives of the three specimen configurations as well as in the time required to form cracks. Crack propagation rates also differed widely, however, the number of cracks observed in the fusion welded test panels was essentially the same as was seen in the riveted specimens.

The linear cumulative damage theory, even when modified by the results of constant amplitude box beam tests, was generally unsatisfactory for estimating fatigue life under spectrum loading conditions for any of the specimen configurations. Of five specimens tested under spectrum loading, the linear cumulative damage theory greatly overestimated the fatigue life of three specimens, and underestimated the fatigue lives of the remaining two specimens.

Fatigue Crack Behavior.- Although cracks appeared in the same order and locations in both the spotwelded and riveted box beam specimens, this was not true for those specimens fabricated through the use of fusion welding. This difference in bahavior is attributed to the lack of well-defined areas of stress concentration in a typical fusion welded structure.

As noted earlier, at the time a crack length of 0.50 inch was attained, the spotwelded specimens contained more cracks than either the riveted or fusion welded specimens.

Crack growth behavior in all specimen configurations was generally similar in that initial growth occurred at a fairly uniform rate up to a crack length of 0.25 to 0.50 inch at which time an increase in overall growth rate was observed. Also noted was a tendency for the majority of cracks in any individual specimen to propagate at rates which were essentially the same. The crack propagation rates observed in the spotwelded specimens, however, were higher than those seen in either the riveted or fusion welded specimens.

The crack propagation rates in the fusion welded panels were comparable to those seen in the riveted panels reported in reference (1). However, the integrally stiffened arrangement resulting from this method of construction proved unable to retard crack growth and, additionally in those areas where appreciable crack growth was seen, the stiffeners themselves suffered considerable damage due to cracking. This is opposed to the results reported in reference (1) where extensive cracking of the skin panels failed to produce damage in either stiffeners or doublers.

The fact that some cracks appeared suddenly in two of the fusion welded specimens points to a need for detailed investigations into welding and/or heat treatment processes to eliminate this behavior. This is particularly true in the case of weld repairs which tend to induce high local residual stresses.

CONCLUSIONS

Four skin-stringer panels were fabricated through the use of fusion welding techniques. One panel was fatigue tested at room temperature with S_{max} = 25 000 psi and S_{min} = -12 500 psi, one panel was fatigue tested at 550°F with S_{mean} = 41 250 psi and S_{alt} = $\pm$6 250 psi, the remaining two panels were tested under spectrum loading with S_{lgD} = 25 000 psi.

1. The constant amplitude fatigue lives of the fusion welded specimens were generally greater than those of either the riveted or the spotwelded specimens. There was no correlation between fatigue life and specimen type when subjected to spectrum loading.

2. In the fusion welded specimens the initial crack location was random in nature and not related to specimen geometry, however, the initial crack location in both spotwelded and riveted test specimens was the same in all tests.

3. Cracking in the fusion welded specimens was confined to longitudinally oriented welds.

4. Flaw sites, determined by X-ray inspection, did not correlate with fatigue damage sites observed during testing.

5. Both slow growing cracks, which were confined to the weld zone, and fast growing cracks, which propagated out of the weld zone, were observed during the tests on fusion welded specimens. Approximately 80 percent of the cracks seen in the fusion welded specimens were of the slow growing type. The remaining 20 percent had crack growth rates which were comparable to those seen in the riveted specimens tested earlier and which were as low as one-fourth of the rates observed in the spotwelded specimens.

6. Fatigue cracks in the fusion welded specimens propagated in both the skin and stiffeners as opposed to the cracks in the spotwelded and riveted specimens which were confined to the skin.

7. The number of cracks observed in the fusion welded specimens were comparable to the number seen in the riveted specimens and about one-third the number seen in the spotwelded specimens.

8. The linear cumulative damage theory, modified by the results obtained during constant amplitude tests, failed to provide realistic estimates of fatigue life for the fusion welded, spotwelded and riveted specimens.

APPENDIX A

FABRICATION OF FUSION WELDED TEST SPECIMENS

Summary - In order that the fatigue behavior of a representative fusion welded structure might be evaluated and compared with that of structures fabricated by more conventional means, the fusion welded panels described herein were fabricated for use on this program. To avoid compromise of the primary program objectives, "state-of-the-art" welding processes were employed throughout this phase of the program.

Butt fusion welding (both manual and automatic) processes as well as burn-thru fusion welding techniques were employed to fabricate the specimens for this program. All welds received a 100% radiographic inspection prior to acceptance and, wherever necessary, repairs were made to eliminate defects such as excess porosity, heavy metal inclusions, incomplete fusion, etc. Subsequent to final acceptance of the welded panels, all weld beads were ground flush and the panel was machined to final size before delivering to the laboratory for mating to the test fixture.

The following paragraphs contain a brief description of the tooling and fabrication procedures utilized during this program.

Stiffener Fabrication - Stiffeners, 120 inches long, were fabricated by butt welding two 60 inch long segments. These segments were brake formed to the desired dimensions and the ends were machined square. Stiffener segments were then hand matched to provide the best possible fit and marked for future identification. This operation was made necessary by the slight variations in spring back normally encountered in a group of supposedly identical pieces.

A plastic bubble enclosure with a suitable base and insertion openings for the stiffener segments was fabricated to provide an inert gas (argon) atmosphere. Copper chill bars, with back-up gas provisions, were also provided.

All parts, including the chill bars, were cleaned prior to welding, inserted into the plastic bubble and clamped to provide the proper register between mated parts. After vacuum purging of the system to remove atmospheric contamination, a positive flow of argon was admitted into the enclosure to prevent aspiration of additional contaminants. The stiffener segments were then joined by manual TIG welding. Low interstitial Ti-8Al-1Mo-1V filler wire was used during this operation to prevent thinning at the weld joint.

Subsequent to completion of the welding operations, the stiffener weld joints were radiographically inspected, defects were repaired, and the weld beads were ground flush. The stiffener to skin attachment leg of each stiffener was then machined to match the inner surface of the skin panels as required. Hand fitting was employed whenever necessary to insure the best possible fit and each stiffener was coded to identify panel and location.

Skin Panel Joining - The basic skin panel for this specimen consisted of two 24 by 65 inch sections which were chem-milled for doublers and pads. These panels were then joined by a butt fusion weld near the panel centerline. See Figures 3 through 6.

A thirty-six inch long air clamp type welding tool was utilized for joining the two panel segments. This tool incorporated copper chill bars and provisions for supplying an inert gas atmosphere to the underside of the weld. A sketch showing the pertinent details of this tool is presented in Figure 26.

The panel segments were joined through the use of automatic TIG welding techniques. Prior to welding the ends of the members to be joined were machined, solvent cleaned and draw filed. After insertion in the welding fixture, the panels were welded using the weld schedule outlined below:

Weld Schedule for Joining Panel Details

Material	Ti-8Al-1Mo-1V Duplex Annealed
Gage	0.100 inch to 0.100 inch
Wire Type	Ti-8Al-1Mo-1V, ELI
Joint Type	Square Butt
Weld Tool Type	Air Clamping
Joint Preparation	Machined and Draw Filed
Cleaning	Power Sand, Hand Sand, MEK Wipe
Back-up Groove Width	0.187 inch
Back-up Groove Depth	0.050 inch
Hold-down Clamp Nose Height	0.125 inch
Hold-down Clamp Spacing	0.312 inch
Filler Wire Diameter	0.045 inch
Filler Wire Feed Rate	16 inches/minute
Torch Gas Cup Size	5/8 inch ID
Electrode Size and Point	1/8 - 90°
Electrode Extension	0.450 inch
Torch Gas and Flow	Hilium -40 cfh
Back-up Gas and Flow	Argon - 20 cfh
Shielding Gas and Flow	Argon - 20 cfh
Volts	11
Amperes	210
Welding Speed	5.5 inches/minute

Although radiographic inspection failed to reveal the presence of any rejectable defects in the joined panel details, visual inspection revealed the presence of one small area of local thinning on specimen number 1. The exact cause of this defect is not known, but it probably resulted from poor chill bar contact in this area. The resultant thinning, 5 to 10 percent of the net thickness, was within normal sheet tolerances and was considered to be relatively minor. However, a decision was made to repair weld this area thus affording an opportunity to observe the behavior of a repaired area under fatigue loading.

The area to be repaired was ground slightly and cleaned in preparation for the repair operation. This repair was accomplished by manual TIG welding in an inert gas filled plastic bubble.

Upon completion of these welding operations, all weld beads were ground flush, top and bottom, in preparation for the final welding operations.

Final Specimen Assembly - During final assembly of the test specimens it was necessary that five stiffeners be attached to the basic skin panels in accordance with the drawing of Figure 2. A prime requisite for this operation was the precise location of the stiffeners to insure compatibility with the existing box-beam test fixture shown in Figure 7. Appropriate tooling and welding sequences were developed to meet this requirement.

A twelve-foot long air clamping hold-down tool, which was available from an earlier production program, was selected for use during this program. Appropriate modifications were made to this tool to permit stiffener welding. A back-up bar, containing provisions for sealing the underside of the weld area as well as provide a suitable inert atmosphere, was made to fit this air clamp tool. Removable inserts were incorporated in this back-up bar to accommodate all stiffener and/or panel orientations thus obviating the need for separate tooling for each stiffener attachment. Special indexing devices were also incorporated in this tool to facilitate stiffener positioning. A schematic showing the general arrangement of this welding fixture is shown in Figure 27.

Stiffeners were joined to the skin panels through the use of a two-pass TIG welding process. The initial pass, made without the addition of filler wire, was a penetration pass to join the stiffener to the skin panel and form the desired fillets at the junction of the two members. The second pass was a fusion pass during which time filler wire was added to fill the skin concavity left by the initial weld pass and furnish weld bead reinforcement. Automatic TIG welding techniques were employed to accomplish this task. In those areas were the skin thickness was increased to provide local reinforcement, see Figures 4 and 6, the heat input was manually controlled by a reduction of torch travel speed and an increase in welding current to insure adequate penetration. The stiffener to skin welds were made in accordance with the following weld schedule:

Weld Schedule for Stiffener to Skin Welding

(All material used was Ti-8Al-1Mo-1V, Duplex Annealed)

	First Pass		Second Pass
Skin Gage	0.100 (basic)	0.150 (steps)	
Stiffener Gage	0.050		
Wire Type	None	None	Ti-8Al-1Mo-1V, ELI
Joint Type	Burn-thru	Burn-thru	Filler
Weld Tool	12 ft air clamp		--
Joint Preparation	Sand, draw file stiffener		
Cleaning	Wet MEK Wipe	--	--
Back-up Groove Width	0.067 Both Sides	--	--
Back-up Groove Depth	0.067	--	--
Hold-down Clamp Nose Height	0.125	--	--
Hold-down Clamp Spacing	0.312	--	0.375
Wire Diameter	None	None	0.045
Wire Feed Rate	--	--	25 ipm
Gas Cup Size	5/8 ID	Same	Same
Electrode Size and Point	1/8 - 90°	Same	Same
Electrode Extension	0.450	0.450	0.450
Torch Gas and Flow	Helium - 35 cfh	Same	Same
Back-up Gas and Flow	Argon - 60 cfh	Same	Same
Shielding Gas and Flow	Argon - 20 cfh	Same	Same
Volts	10-1/4	10-1/4	10-3/4
Current, Amperes	260	290	250
Torch Speed	5.7 ipm	4 ipm	5.7 ipm

Each stiffener weld was subjected to a complete radiographic examination upon completion. Repairs indicated by this inspection were then accomplished before proceeding. No repairs were required due to the presence of either linear or scattered porosity.

There were two types of weld defect which entailed the use of repair procedures to produce an acceptable test panel. These were:

a. Local thinning resulting from insufficient contact between the chill bars and the stock being welded.

b. Heavy metal inclusions which were caused by intermittent malfunctions in the power and/or torch gas supply of the automatic welding equipment.

The repair procedures used to remedy the effects of local thinning were the same as those described earlier in the section on skin panel joining and will not be discussed here.

Heavy metal inclusions were located on the appropriate weld bead by direct measurement from the original X-ray picture of the defect. These inclusions were then either removed or reduced to an acceptable size (0.040 inch maximum diameter) by grinding. Verification of removal was obtained from additional X-ray pictures of the affected area.

Upon satisfactory completion of the grinding operation, the panel was cleaned and reinstalled in the welding fixture for repairs. Initially, the ground-out area resulting from removal of the heavy metal inclusion was filled through the use of the manual controls on the welding equipment. These areas usually required the addition of a significant amount of filler material due to the depth of the ground-out areas. In order to assure adequate fusion between the repair weld and the adjacent material as well as to minimize the high local residual stresses which would be expected from this procedure, an additional fusion pass (without filler wire) was executed over the entire length of the weld. After completion of repairs the entire weld was again X-ray inspected before proceeding.

As noted earlier, one crack which was observed during the test of specimen number 1, was repaired in order to permit test continuation. This repair was accomplished while the test specimen was still mounted on the test fixture as described below.

One side of the box-beam fixture was removed to provide access to the lower side of the test specimen. An inspection made at this time confirmed that the damage was confined to an area of the panel having a nominal thickness of 0.050 inch and did not extend into any of the chem-milled pads. Following this inspection, the damaged area was then removed by grinding.

Since the use of a plastic bubble on the back side of the damaged area was not possible, a special tool was fabricated to furnish the required back-side protection. This tool, which was fitted between the stiffeners on either side of the crack, contained provisions for the flow of the desired inert gas (argon) over the back of the weld as well as seals which effectively isolated this area from the surrounding atmosphere. A copper chill-bar was machined to surround the repair area on the exposed, or upper, surface of the test specimen after which a plastic bubble was placed over the area. Manual TIG welding techniques were then used to effect the desired repair. After X-ray examination, the repair weld was ground flush inside and out and the test was continued.

Panel Machining.- After completion of all welding operations, all external weld beads were removed by grinding and hand sanding.

The final machining operations on the panels involved cutting the door opening and circular cut-outs thru the skin as shown in Figures 4 and 5 followed by the necessary trimming to prepare the panel for mating to the test fixture. Since the actual machining operations were typical of those used for machining titanium, a description of these operations will not be presented.

However, panel distortion created some difficulties in that special holding fixtures were required to reduce time and handling operations during final machining.

Problem Areas - Although the required welding operations were accomplished with little difficulty, and basic weld tooling performed satisfactorily, there were two areas in which problems occurred which warrant further consideration. These are:

a. Repair welding techniques
b. Panel warpage

Since it is impossible to fabricate a perfect welded structure, there are two basic items which are deserving of further consideration. First, it is essential that the influence of typical weld defects such as porosity, heavy metal inclusions, micro-cracks, incomplete fusion, etc., be thoroughly understood in order to minimize the incidence of scrappage and/or costly repair operations. Second, once the criteria for flaw rejection are established, it is necessary that economical procedures be developed for the repair of such defects. The behavior of repair welds during the course of this program (see the discussion of test specimen number 1 earlier in this report) points to this need.

Panel distortion, which is caused by weld shrinkage induced stresses, is a problem which requires further investigation. Although stress relief is almost universally accepted as a means of reducing residual stresses to an acceptable level, this is often impractical on a large structure. Further studies are, therefore, recommended to establish the magnitude of these residual stresses, their overall effect on structural behavior and, in addition, to assess the effectiveness of varied welding techniques in reducing these stresses to an acceptable level.

APPENDIX B

RESULTS OF STUDIES TO ESTABLISH A RELATIONSHIP BETWEEN THE FATIGUE BEHAVIOR OF DUPLEX ANNEALED AND TRIPLEX ANNEALED Ti-8Al-1Mo-1V

One of the basic objectives of this investigation was to make a direct comparison of the structural fatigue behavior of similar structures which were fabricated by different methods. With this objective in mind, the material originally chosen for specimen fabrication on this program was the same as that used during the programs reported in references (1) and (2), namely, Ti-8Al-1Mo-1V in the triplex annealed condition. At the time of ordering those materials which were required for specimen fabrication, it was learned that Ti-8Al-1Mo-1V was no longer being produced in the triplex annealed condition. The program was then redirected to employ this material in the duplex annealed condition.

Since a direct comparison between the results reported herein and those contained in reference (1) was no longer possible, a study was initiated in an attempt to establish a base line from which rational fatigue life comparisons could be made. The data which were ultimately used to conduct this study are summarized in references (2) and (3) for triplex annealed material, and in reference (4) for duplex annealed material.

Initial comparisons were made between the basic tensile properties of each material in both the unwelded and fusion welded conditions. These comparisons are summarized in Figures 28 and 29 in which it can be seen that no unusual behavior patterns are evident for either material condition, and further that the transverse weld strength is not influenced by the initial heat treatment of the base material.

Similar comparisons, which were made using the fatigue data contained in references (2), (3) and (4), were made and are summarized in Figures 30 and 31. It should be noted at this time that in addition to the normal scatter which would normally reflect differences in fabrication practices and/or testing techniques used at different laboratories and the often subtle differences in behavior between apparently identical weld samples, the lack of commonality between the test conditions used at the different laboratories undoubtedly contributed to any differences noted.

Figure 30 is a non-dimensionalized plot containing base metal, unnotched fatigue data from the subject references from which it can be seen that the data are in reasonable agreement, particularly in the case of references (3) and (4), thus indicating that on the basis of S_{max}/S_{tu}, both the duplex and triplex annealed Ti-8Al-1Mo-1V would be expected to behave in a similar manner.

It was not possible to establish the same degree of agreement between the transverse fusion weld data contained in references (2) and (4). In addition, since the skin-stringer panels tested during this investigation had over 90% of their welds oriented in a direction parallel to the applied load, the lack of published data on longitudinal fusion welds further complicated the problem.

Since the fusion welded specimens which were tested during the program reported in reference (2) were not representative of the best welds attainable, and in view of the excellent agreement in parent metal behavior demonstrated by the data from references (3) and (4), it was assumed that the transverse fusion weld curves contained in reference (4) would be applicable to either duplex or triplex annealed Ti-8Al-1Mo-1V when used on the basis of S_{max}/S_{tu}.

As mentioned earlier, the critical welds in the specimens tested during the course of this investigation were parallel to the direction of applied load, a condition for which little if any published fatigue data are available. In an effort to establish base line data which would be useful in analysis of the program test results, the weld fatigue curves contained in reference (2) were used as a guide. Although these data are somewhat doubtful when considered on a quantitative basis, the general relationship between the performance of the transverse and longitudinal welds as seen from these data is considered realistic. Using this relationship and the transverse fusion weld fatigue life curves contained in reference (4), tentative fatigue life curves for longitudinally oriented fusion welds were then constructed. These curves are presented in non-dimensional form as Figure 32 to this report.

REFERENCES

1. Peterson, J. J.: Fatigue Behavior of Ti-8Al-1Mo-1V Sheet in a Simulated Wing Structure under the Environment of a Supersonic Transport. NASA CR-333, November 1965.

2. Peterson, J. J.: Fatigue Behavior of AM-350 Stainless Steel and Titanium 8Al-1Mo-1V Sheet at Room Temperature, 550°F and 800°F. NASA CR-23, May 1964.

3. Gideon, D. N.; Marshall, C. W.; Holden, F. C.; and Hyler, W. S.; Exploratory Studies of Mechanical Cycling Fatigue Behavior of Materials for the Supersonic Transport, NASA CR-28, April 1964.

4. McCulloch, A. J.: and Young, L.: Fatigue Behavior of Sheet Materials for the Supersonic Transport, AFML-TR-64-399, January 1965.

TABLE I

RESULTS OF MECHANICAL PROPERTY TESTS
Ti-8Al-1Mo-1V DUPLEX ANNEALED

No.	t nom.	Grain Dir.	Type Spec.	Stu ksi	Sty ksi	% elong 2" G.L.	E ksix10^{-3}
			ROOM TEMPERATURE				
1	0.100	L	(a)	150.0	143.6	15.0	17.5
2	0.100	L	(a)	149.8	143.6	14.1	17.6
5	0.150	L	(a)	148.3	142.8	13.6	16.4
6	0.150	L	(a)	149.2	145.3	13.7	16.6
9	0.050	L	(a)	149.6	144.8	14.1	17.6
10	0.050	L	(a)	152.7	145.5	13.9	17.2
13	0.050	L	(b)	156.3	-	7.2(c)	-
14	0.050	L	(b)	153.5	-	12.1(d)	-
15	0.050	L	(b)	154.5	-	8.2(c)	-
			550°F				
19	0.100	L	(a)	115.0	101.4	17.5(e)	-
20	0.100	L	(a)	113.7	100.8	15.3(e)	-
21	0.150	L	(a)	114.6	99.9	15.9	-
22	0.150	L	(a)	112.1	93.8	16.6(e)	-
23	0.050	L	(a)	116.1	102.8	13.2(e)	-
24	0.050	L	(a)	119.4	104.8	13.2	
16	0.050	L	(b)	122.4	-	12.8(d)	-
17	0.050	L	(b)	119.9	-	10.4(d)	-
18	0.050	L	(b)	121.8	-	12.0(d)	-

NOTES:

a. Parent metal specimen.
b. Transverse fusion weld (as welded, weld bead machined flush)
c. Failed in weld metal.
d. Failed in parent metal.
e. Failed outside middle third of test section.

TABLE II

CUMULATIVE FREQUENCIES OF COMBINED GUST AND MANEUVER LOADS

(12000 Operational Flights and 500 check Flights)

	Climb		Cruise		Check Flt.	
θ	Total	Block	Total	Block	Total	Block
0.25	78 000.0	1 560.00	3000.0	60.00	11 500.0	230.00
0.35	13 200.0	264.00	552.0	11.04	2 800.0	56.00
0.45	3 120.0	62.40	84.0	1.68	1 000.0	20.00
0.55	670.0	13.40	8.4	0.17	300.0	6.00
0.65	145.0	2.90			75.0	1.50
0.75	40.0	0.80			15.0	0.30
0.85	18.0	0.36				
0.95	9.0	0.18				
1.05	4.0	0.08				
1.15	2.5	0.05				
G.A.G.	12 000.0	240.00			3 500.0	70.00

NOTES:

1. G.A.G. cycle for operational flights varies from $-0.5\ S_{19_D}$ to $+1.0\ S_{19_D}$
2. G.A.G. cycle for check flights varies from $-0.5\ S_{19_D}$ to $+0.7\ S_{19_D}$
3. Mean stress for climb loads = $(1.0)\ (S_{19_D})$
4. Mean stress for cruise loads = $(0.75)\ (S_{19_D}) + (0.65)(S_{19_D})$
5. Mean stress for check flights = $(0.70)(S_{19_D})$
6. θ defines the alternating stress component of load: $S_{alt} = \theta S_{19_D}$
7. $S_{19_D} = 25\ 000$ psi.
8. Loads incurred during descent not included, below endurance limit.

TABLE III

PROOF LOAD STRAIN GAGE READINGS,
SPECIMEN NUMBER 1

Gage No.	Locat. Y - in. Z - in.	Actuator Load-Pounds 5 000	7 500	10 000	12 500	15 000	17 500	20 000
		ϵ (a)	ϵ	ϵ	ϵ	ϵ	ϵ	ϵ
		S (b)	S	S	S	S	S	S
1	-20.1	225	330	440	550	660	780	890
	4.30	3 900	5 700	7 700	9 600	11 500	13 600	15 500
2	-20.1	240	350	470	590	710	830	940
	7.85	4 200	6 100	8 200	10 300	12 400	14 400	16 400
3	-20.1	230	360	480	590	710	830	950
	11.10	4 200	6 300	8 300	10 300	12 400	14 400	16 600
4	-20.1	230	350	470	590	710	830	950
	14.65	4 000	6 100	8 200	10 300	12 400	14 400	16 600
5	-20.1	220	330	440	550	660	780	900
	18.20	3 800	5 700	7 700	9 600	11 500	13 600	15 700
7	- 0.75	240	350	480	590	710	840	950
	7.85	4 200	6 100	8 300	10 300	12 400	14 600	16 600
9	-0.75	180	270	370	460	560	650	740
	14.65	3 100	4 700	6 400	8 000	9 700	11 300	12 900
10	-0.75	280	420	570	710	860	1 010	1 140
	18.20	4 900	7 300	9 900	12 400	14 900	17 600	19 800
11	+22.0	200	305	410	510	620	720	820
	4.30	3 500	5 300	7 100	8 900	10 800	12 500	14 300
12	+22.0	200	290	390	490	590	690	785
	7.85	3 500	5 000	6 800	8 500	10 300	12 000	13 700
14	+22.0	200	300	405	510	620	730	820
	14.65	3 500	5 200	7 100	8 900	10 800	12 700	14 300
15	+22.0	190	290	380	480	580	685	785
	18.20	3 300	5 000	6 600	8 300	10 100	11 900	13 700
16	-20.1	340	520	700	870	1 050	1 215	1 400
	12.00	6 000	9 100	12 300	15 300	18 400	21 400	24 600
17	+22.0	395	590	780	975	1 170	1 385	1 560
	12.40	6 500	9 700	12 900	16 100	19 300	22 800	25 700
30	-2.0	400	600	800	1 000	1 200	1 400	1 600
	12.40	7 000	10 500	14 100	17 600	21 100	24 600	28 100
31	-2.0	400	590	785	985	1 170	1 360	1 560
	9.47	7 000	10 400	13 800	17 300	20 600	23 900	27 400

NOTES:

a. ϵ shown in micro-inches/inch.

b. S shown in psi.

1. Gages 1 through 15 located on underside of stiffener flange.
2. Gages 6, 8 and 13 damaged, no readings recorded.

TABLE IV

INSPECTION LOG FOR SPECIMEN NUMBER 1

Constant Amplitude, RT, GAG
S_{max}=25 ksi, S_{min}= -12.5 ksi
Crack lengths shown in inches

Crack Number	Location (a) Y-in.	Location (a) Z-in.	Cycles 19 266	21 233	22 242	24 230	26 232	28 250
1	-1.10	+9.36	0.90	(b)				
2	+4.17	+14.10		0.22	0.22	0.24	0.24	0.24
3	+4.32	+14.00		.075	.09	.115	.115	.14

Crack Number	Location Y-in.	Location Z-in.	Cycles 29 087	29 659	31 564	31 972	32 749	33 929
1			(b)					
2			0.25	0.25	0.35	0.43	0.48	0.54
3			.15	.15	.19	.20	.21	.25
4	-21.17	+8.42	.23	.26	.31	.35	.37	.43
5	-13.6	+14.19						.14(c)

Crack Number	Location Y-in.	Location Z-in.	Cycles 35 336	36 836	37 939	39 092	40 177	41 698
1			(b)					
2			0.63	0.83	0.99	1.11	1.25	1.56
3			.32	.46	.565	.725	.835	1.16
4			.54	.82	1.05(d)	1.33	1.45	1.90
5			.37	.71	.97(e)	1.14	1.35	1.56

Crack Number	Location Y-in.	Location Z-in.	Cycles 42 920	43 261	44 453	46 248	47 309	48 359
1			(b)					
2			1.73	1.81	1.96	2.18	2.32	2.53(g)
3			1.33	1.36	1.52	1.79	1.87	2.02(g)
4			2.17	2.32	2.63	3.04	3.44	3.61
5			1.77	1.86	2.17	2.42	2.63	2.89
6	+1.8	+8.21		.21	.27	.49	.67	1.00
7	-7.15	+14.14					(f)	(f)
8	-14.28	+14.09					.08	.08

TABLE IV (Concluded)

INSPECTION LOG FOR SPECIMEN NUMBER 1

Crack Number	Location		Cycles					
	Y-in.	Z-in.	49 258	50 316	51 346	52 436	52 877	
1	-1.10	+9.36	(b)					
2	+4.17	+14.10	2.65	2.79	2.85	3.01	3.08	
3	+4.32	+14.00	2.17	2.24	2.28	2.54	2.62	
4	-21.17	+8.42	3.75	3.92	4.48	5.76	6.14(i)	
5	-13.6	+14.19	3.02	3.17	3.35(h)	3.54	3.61	
6	+1.8	+8.21	1.25	1.46	1.64	2.03	2.13	
7	-7.15	+14.14	(f)	(f)	0.14	.14	.17	
8	-14.28	+14.09	0.08	.08	0.08	.08	.08	
9	-18.68	+8.4	0.11	.13	0.14	.14	.14	
10	-10.90	+8.4	0.10	.12	0.15	.15	.18	
11	+5.12	+10.8			0.16	.20	.22	

NOTES:

(a) Coordinates show the location of the crack origin at detection.

(b) Crack No. 1 repair welded after 19 266 cycles and showed no further damage.

(c) Crack No. 5 entered stiffener leg at 33 929 cycles.

(d) Crack No. 4 entered stiffener leg at 37 939 cycles.

(e) Crack No. 5 entered cut-out at 37 226 cycles.

(f) Strain deformation only.

(g) Stiffener under cracks 2 and 3 severed at 47 558 cycles.

(h) Stiffener at crack number 5 severed at 50 674 cycles.

(i) At conclusion of test, crack number 4 was approximately 1.0 inch into stiffener leg at Z = +10.61.

TABLE V

INSPECTION LOG FOR SPECIMEN NUMBER 3

Spectrum, RT and 550°F, $S_{1_{gp}}$=25 ksi
Crack Lengths Shown in Inches

Crack Number	Location (a)		Flights					
	Y-in.	Z-in.	5 250	5 500	5 750	6 000	6 250	6 500
1	-2.09	+17.5	0.04	0.04	0.06	0.06	0.06	0.06
2	-4.55	+14.1	.04	.04	.04	.04	.04	.06
3	+16.55	+17.5	.06	.06	.08	.10	.10	.10
4	-12.60	+17.5		.02	.02	.02	.02	.02
5	+0.45	+10.5		.02	.02	.02	.02	.04

Crack Number	Location							
	Y- in.	Z-in.	6 750	7 000	7 250	7 500	7 750	8 000
1			0.06	0.06	0.06	0.06	0.06	0.06
2			.06	.06	.06	.06	.06	.06
3			.10	.10	.10	.10	.10	.10
4			.02	.04	.04	.04	.04	.04
5			.04	.04	.04	.04	.04	.04
6	+4.5	+4.9						.04

Crack Number	Location							
	Y-in.	Z-in.	8 250	8 500	8 750	9 000	9 250	9 500
1			0.06	0.06	0.08	0.10	0.10	0.10
2			.06	.06	.06	.08	.08	.08
3			.10	.10	.12	.12	.12	.12
4			.04	.04	.04	.04	.04	.04
5			.06	.06	.06	.08	.08	.08
6			.06	.08	.08	.08	.08	.08
7	-18.1	+17.9						.02

TABLE V (Concluded)

INSPECTION LOG FOR SPECIMEN NUMBER 3

Crack Number	Location		Flights					
	Y-in.	Z-in.	9 750	10 000	10 250	10 500	10 750	11 000
1			0.10	0.10	0.10	0.10	0.10	0.10
2			.08	.08	.08	.08	.08	.08
3			.12	.12	.12	.12	.12	.12
4			.04	.04	.04	.04	.04	.04
5			.08	.08	.08	.08	.08	.08
6			.08	.08	.08	.08	.08	.08
7			.02	.02	.02	.02	.02	.02
8	+4.8	+17.7			.02	.02	.02	.02
9	-21.15	+17.7						.02

Crack Number	Location		Flights					
	Y-in.	Z-in.	11 250	11 500	11 750	12 000	12 250	12 500
1	-2.09	+17.5	0.10	0.12	0.12	0.12	0.12	0.12
2	-4.55	+14.1	.08	.08	.08	.08	.08	.08
3	+16.55	+17.5	.14	.14	.14	.14	.16	.16
4	-12.60	+17.5	.04	.06	.06	.06	.06	.06
5	+0.45	+10.5	.08	.08	.08	.08	.08	.08
6	+4.5	+4.9	.08	.08	.08	.10	.10	.10
7	-18.1	+17.9	.02	.02	.02	.02	.02	.02
8	+4.8	+17.7	.02	.02	.02	.02	.02	.02
9	-21.15	+17.7	.02	.06	.06	.06	.06	.06
10	+15.05	+17.7						.04
11	-1.0	5.65						.08

NOTE:

(a) Coordinates show the location of the crack origin at detection.

TABLE VI

INSPECTION LOG FOR SPECIMEN NUMBER 4

Spectrum, RT and 550°F, S_{lgD} = 25 ksi
Crack Lengths Shown in Inches

Crack Number	Location (a)		Flights					
	Y-in.	Z-in.	2750	3000	3250	3500	3750	4000
1	+9.35	+ 8.10	0.30(b)	0.32	0.33	0.35	0.36	0.38
2	+5.25	+14.16	.09	.10	.11	.12	.12	.12

Crack Number	Location		Flights					
	Y-in.	Z-in.	4250	4500	4750	5000	5250	5500
1			0.44	0.45	0.45	0.49	0.50	0.53
2			.12	.12	.14	.14	.14	.14
3	+20.1	+8.13				.06	.06	.07
4	+16.2	+5.05				.04	.04	.04
5	+15.6	+4.75				.06	.06	.06
6	-4.94	+4.95				.06	.06	.06
7	-5.82	+4.92				.07	.07	.07
8	+1.34	+8.26				.05	.05	.06

Crack Number	Location		Flights					
	Y-in.	Z-in.	5750	6000	6250	6500	6750	7000
1			0.56	0.58	0.68	0.75	0.80	0.88
2			.16	.16	.16	.16	.16	.17
3			.07	.07	.07	.07	.07	.07
4			.04	.04	.06	.06	.06	.06
5			.06	.06	.06	.06	.06	.06
6			.06	.06	.06	.06	.06	.06
7			.07	.07	.07	.07	.06	.07
8			.06	.06	.06	.06	.06	.06
9	+17.85	+4.70						.04

TABLE VI (Continued)

INSPECTION LOG FOR SPECIMEN NUMBER 4

Crack Number	Location		Flights					
	Y-in.	Z-in.	7250	7500	7750	8000	8250	8500
1			0.96	0.99	1.06	1.11	1.21	1.30
2			.17	.17	.20	.22	.22	.23
3			.08	.08	.08	.08	.08	.08
4			.06	.06	.06	.06	.06	.06
5			.06	.06	.06	.06	.06	.06
6			.06	.06	.06	.06	.06	.06
7			.07	.07	.07	.07	.07	.07
8			.06	.06	.06	.06	.06	.06
9			.04	.04	.04	.04	.04	.04

Crack Number	Location		Flights					
	Y-in.	Z-in.	8750	9000	9250	9500	9750	10 000
1			1.39	1.43	1.57	1.66	1.81	1.88
2			.23	.24	.25	.25	.25	.25
3			.08	.08	.08	.08	.08	.08
4			.06	.08	.08	.08	.08	.08
5			.06	.06	.06	.06	.06	.06
6			.06	.06	.06	.06	.06	.08
7			.07	.09	.09	.09	.09	.11
8			.06	.06	.06	.06	.06	.08
9			.04	.04	.04	.04	.04	.04
10	-13.0	+17.5					.06	.06

Crack Number	Location		Flights					
	Y-in.	Z-in.	10 250	10 500	10 750	11 000	11 250	11 500
1			1.99	2.16	2.32	2.50	2.66	2.81
2			.25	.25	.25	.25	.25	.27
3			.08	.08	.08	.11	.11	.11
4			.08	.08	.08	.06	.06	.06
5			.06	.06	.06	.08	.08	.08
6			.08	.08	.08	.10	.10	.10
7			.11	.11	.11	.14	.14	.14
8			.08	.08	.08	.09	.09	.09
9			.06	.06	.06	.06	.06	.06
10			.06	.06	.06	.06	.06	.06

TABLE VI (Concluded)

INSPECTION LOG FOR SPECIMEN NUMBER 4

Crack Number	Location		Flights					
	Y-in.	Z-in.	11 750	12 000	12 250			
1			2.97	3.28	(c)			
2			.30	.30	0.32			
3			.11	.11	.13			
4			.06	.06	.06			
5			.08	.08	.09			
6			.12	.12	.12			
7			.17	.17	.18			
8			.09	.09	.10			
9			.06	.06	.08			
10			.06	.06	.06			
11	+21.25	+17.5	.04	.04	.06			
12	+21.05	+17.2	.04	.04	.08			
13	+15.36	+17.5			.04			
14	+15.13	+17.5			.04			

NOTES:

(a) Coordinates show location of crack origin at detection.

(b) Crack extends 0.25 inches under door, measurements shown in table are visible lengths only.

(c) Upon completion of the RT portion of this group of flights, crack number 1 had reached a length of 3.45 inches. During the 550°F segment the crack grew rapidly to a length of 6.95 inches. At the conclusion of the test, crack number 1 extended 1.50 inches under the door for a total length of 8.45 inches.

(l) The stiffener at Z = +8.33 was completely severed and the stiffener web at Z = +4.79 was cracked 1.20 inches.

TABLE VII

SUMMARY OF TEST RESULTS, FUSION WELDED, SPOTWELDED AND RIVETED SPECIMENS

	CONSTANT AMPLITUDE ROOM TEMP. S_{max} = 25 Ksi, S_{min} = 12.5 Ksi			CONSTANT AMPLITUDE 550°F S_{max} = 41.25 Ksi, S_{min} = 35 Ksi			SPECTRUM ROOM TEMP. AND 550°F $S_{1_{SD}}$ = 25 Ksi					
	Fusion Welded	Spot Welded	Riveted	Fusion Welded	Spot Welded	Riveted	Fusion Welded		Spot Welded		Riveted	
Predicted Life (Linear Cumulative Damage Theory)	90 000 cyc	13 000 cyc	36 000 cyc	500 000 cyc	75 000 cyc	90 000 cyc	29 000 flts	29 000 flts	3 100 flts	3 100 flts	7 400 flts	7 400 flts
Time to l_c = .03 in.	27 233 cyc (1)	----	8 450 cyc	----	49,000 cyc	41 700 cyc	5 250 flts	2 750 flts (5)	(6)	775 flts (2)	5 600 flts	9 500 flts
Time to l_c = .50 in.	33 250 cyc	25 000 cyc	24 000 cyc	----	80 750 cyc	99 000 cyc	(4)	2 750 flts (5)	-----	1 000 flts (2)	6 815 flts	(4)
Duration of Test	52 877 cyc	33 345 cyc	48 301 cyc	301 364 cyc (3)	159 955 cyc	154 047 cyc	12 500 flts	12 250 flts	-----	2 500 flts	12 500 flts	12 500 flts

NOTES:

1. Crack had attained a length of 0.22 inch prior to detection.
2. Based on extrapolation of test data.
3. Specimen had sustained no damage at this point.
4. No cracks attained a length of 0.50 inch.
5. Crack appeared suddenly between 2500 and 2750 flights.
6. Specimen suffered an instability failure after completion of 1250 flights.

TABLE VIII

COMPARISON OF PREDICTED AND EXPERIMENTAL
BOX BEAM LIVES UNDER SPECTRUM LOADS
(Failure assumed when l_c = 0.50 in.)

← Constant Amplitude Loading →					← Spectrum Loading →				
Spec. No.	Temp °F	Est. Life Cycles (1)	Box Beam Life Cycles	Test Life / Est. Life	Spec. No.	Est. Life Flights (2)	Predicted Life Flights (3)	Test Life Flights	Pred. Life / Test Life
1	80	90 000	33 250	.37	3	29 200	10 800	>12 500	.86
					4	29 200	10 800	2 500	4.32
2	550	500 000	>301 364	>.60	3	29 200	17 600(4)	>12 500	1.41
					4	29 200	17 600(4)	2 500	7.05

NOTES:

1. Constant amplitude life of simple specimens per reference (3).

2. Spectrum life computed according to the linear cumulative damage theory and simple specimen fatigue data contained in reference (3).

3. Box beam predicted life:

$$\text{life} = (\text{computed spectrum life}) \times \frac{\text{Constant amplitude box beam life}}{\text{Constant amplitude simple specimen life}}$$

4. The lack of fatigue damage in specimen number 2 makes this prediction unreliable, these data included for reference only.

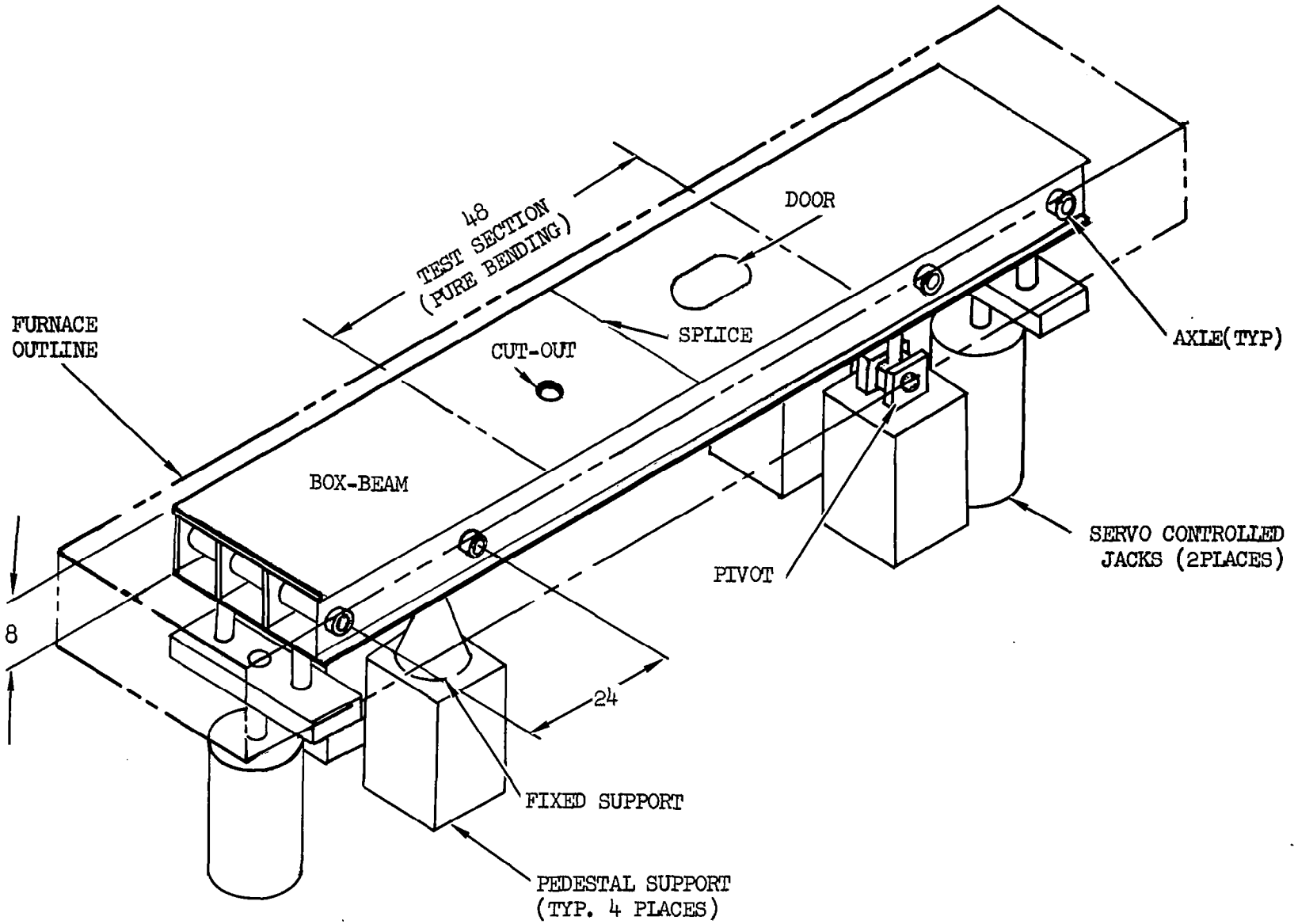

Figure 1. Sketch Showing General Arrangement of Box Beam and Loading Arrangement

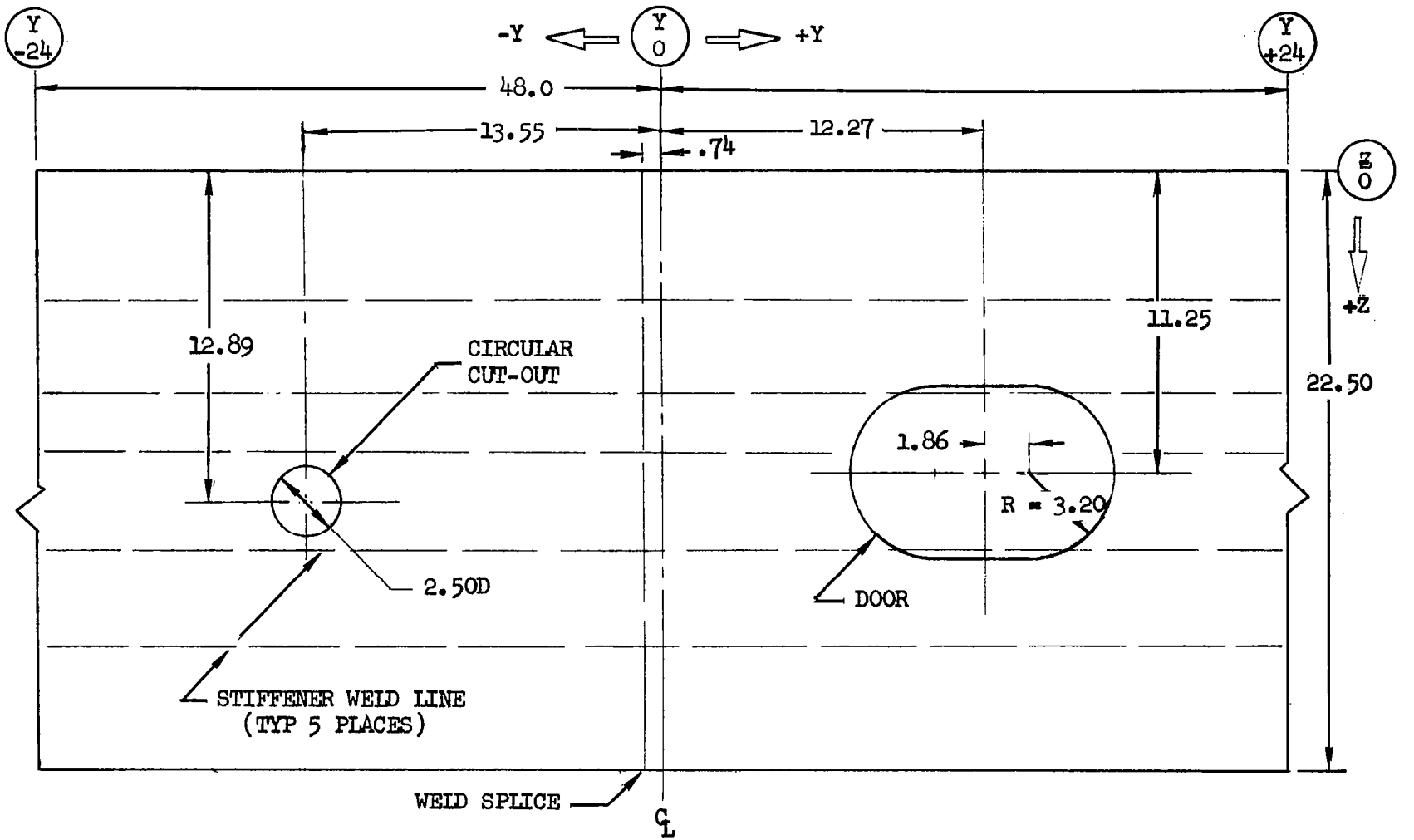

Figure 2. General Arrangement of Test Specimen

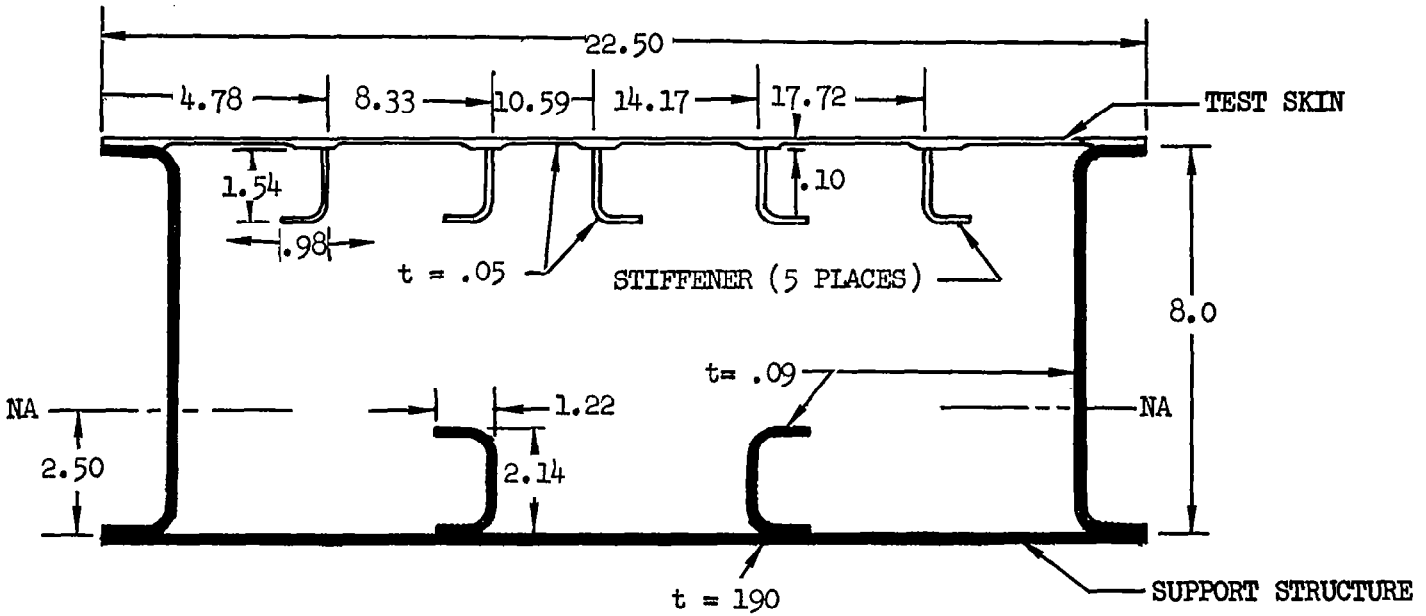

TYPICAL SECTION THRU SKIN-BOX ASSEMBLY

Figure 2. General Arrangement of Test Specimen (Concluded)

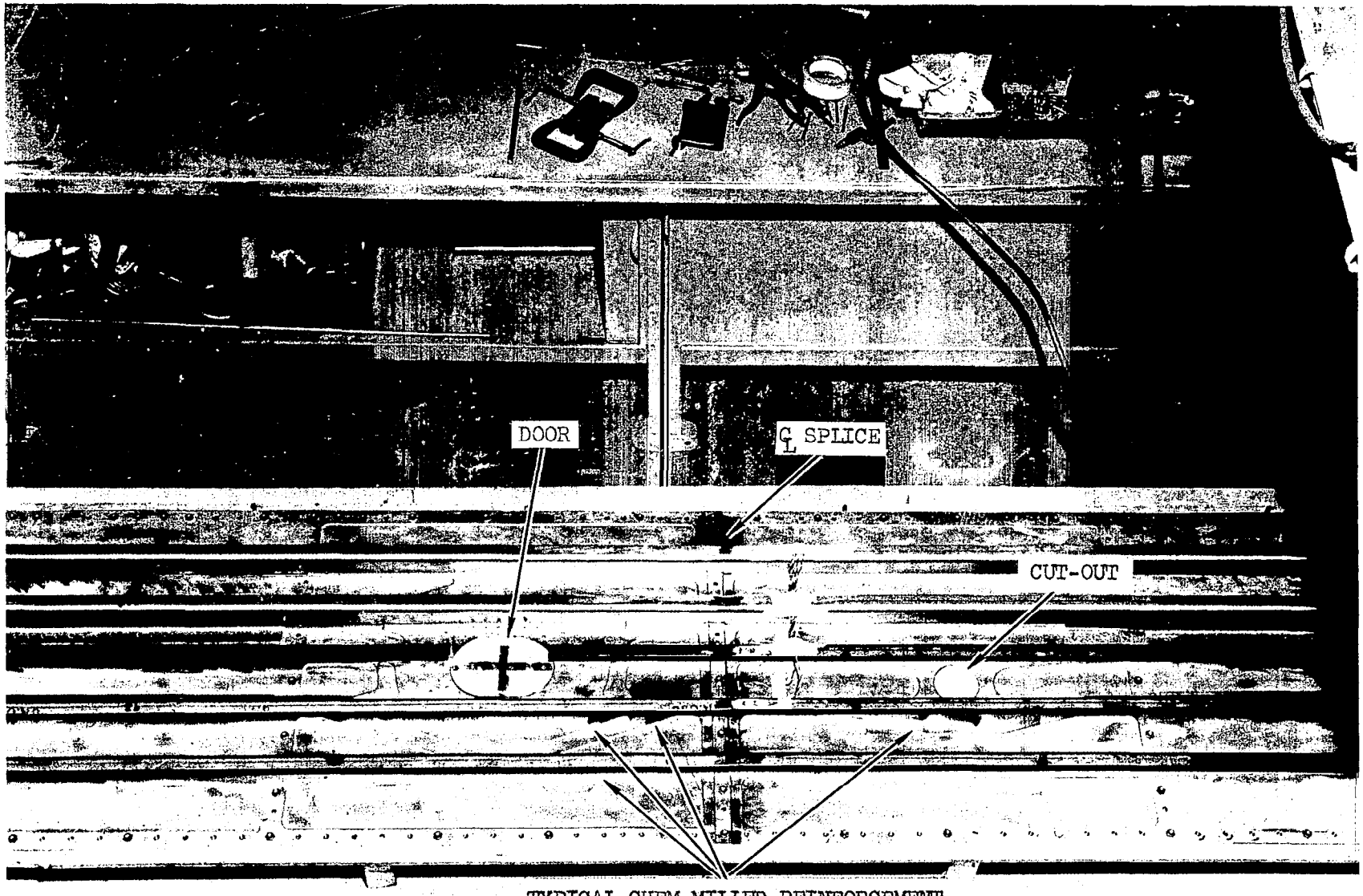

Figure 3. General Internal Arrangement of Fusion Welded Skin Test

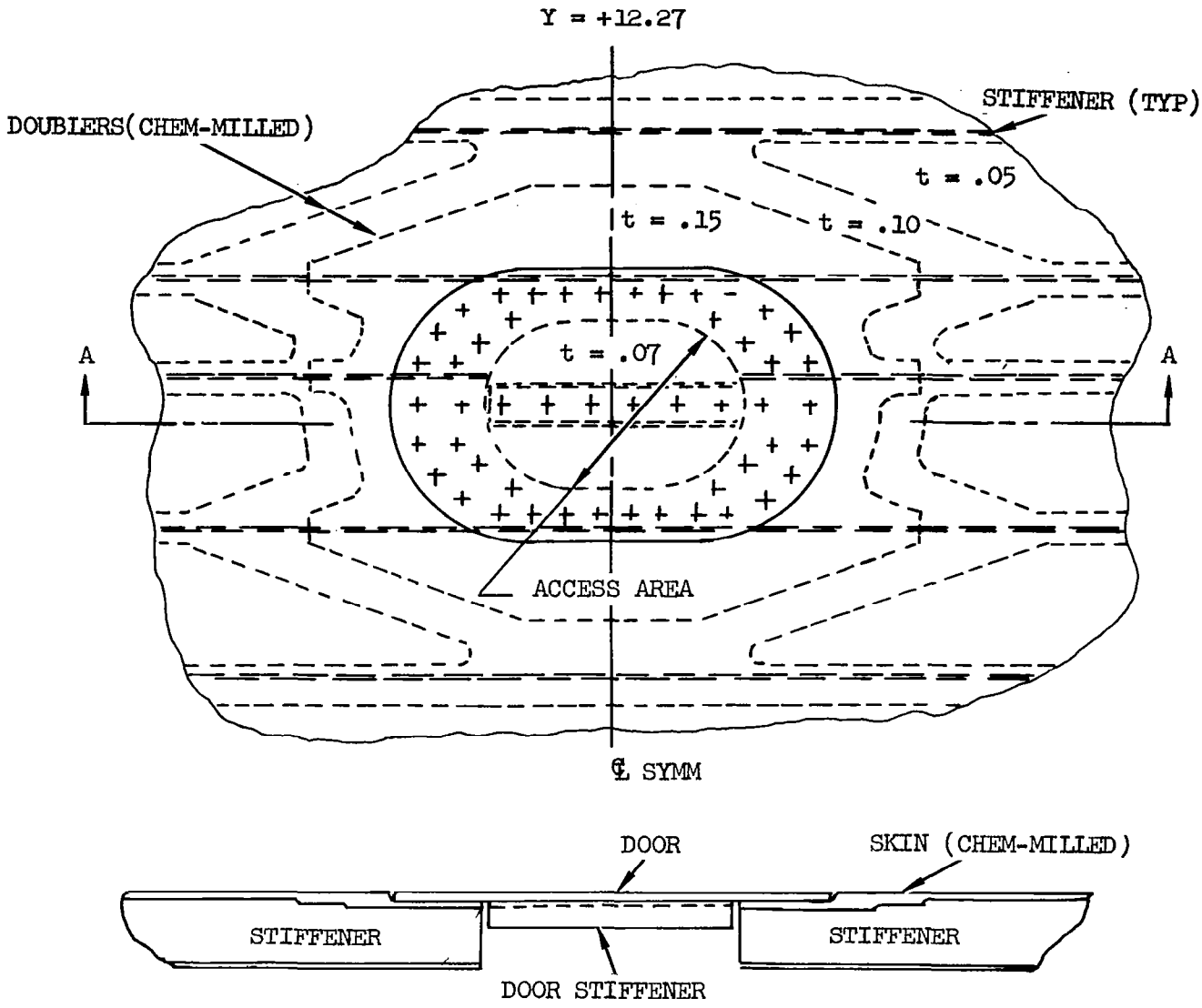

SECTION A-A

NOTES:

1. ALL STOCK, Ti-8Al-1Mo-1V, DUPLEX ANNEALED
2. DOOR SYMMETRICAL ABOUT 2 AXES
3. DOUBLERS SYMMETRICAL ABOUT 1 AXIS

Figure 4. Sketch Showing Details of Structural Door

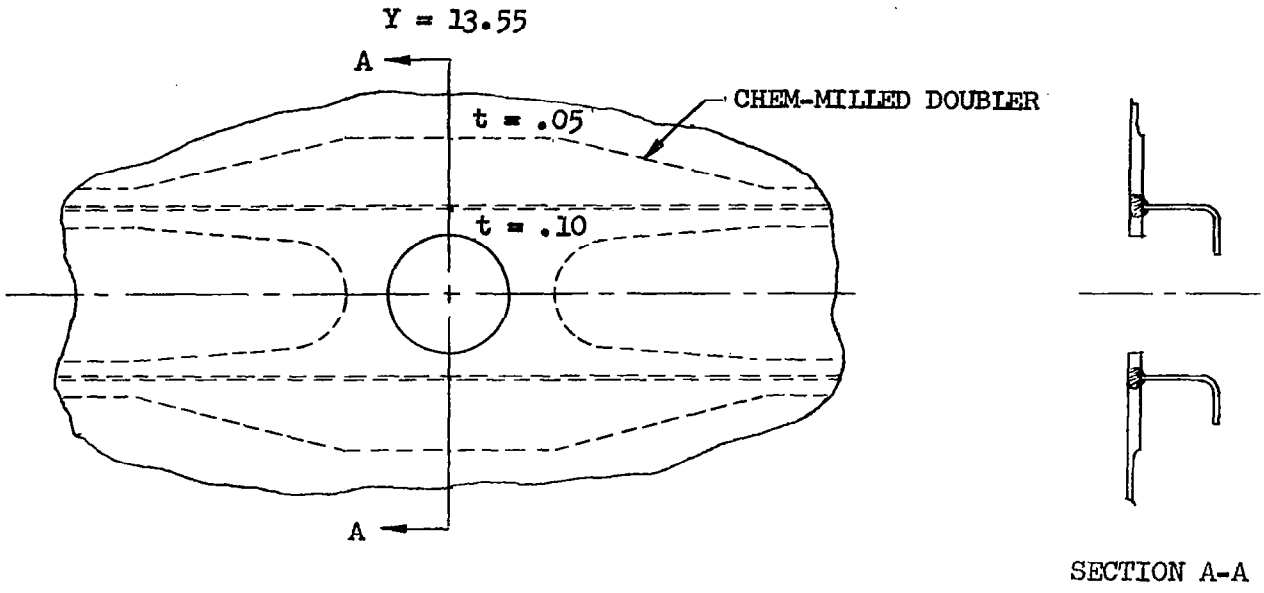

Figure 5. Sketch Showing Details of Circular Cut-out

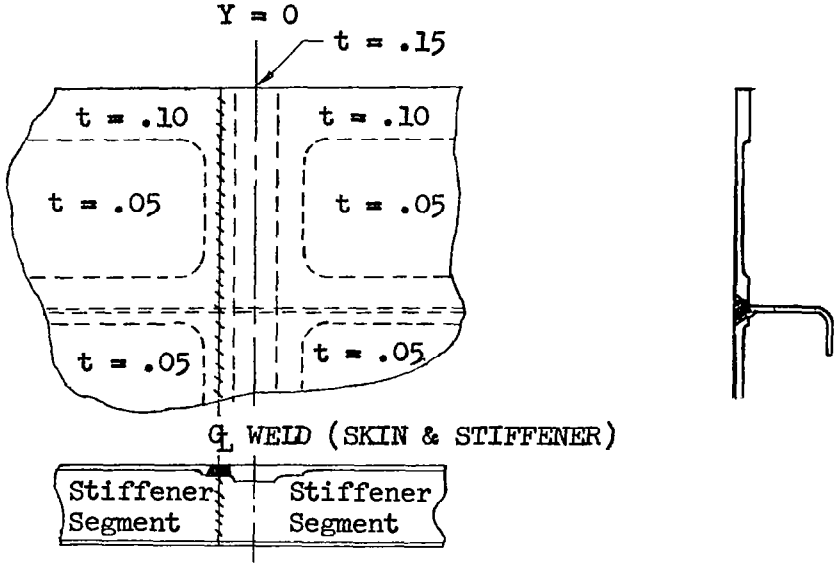

Figure 6. Sketch Showing Details of Centerline Splice

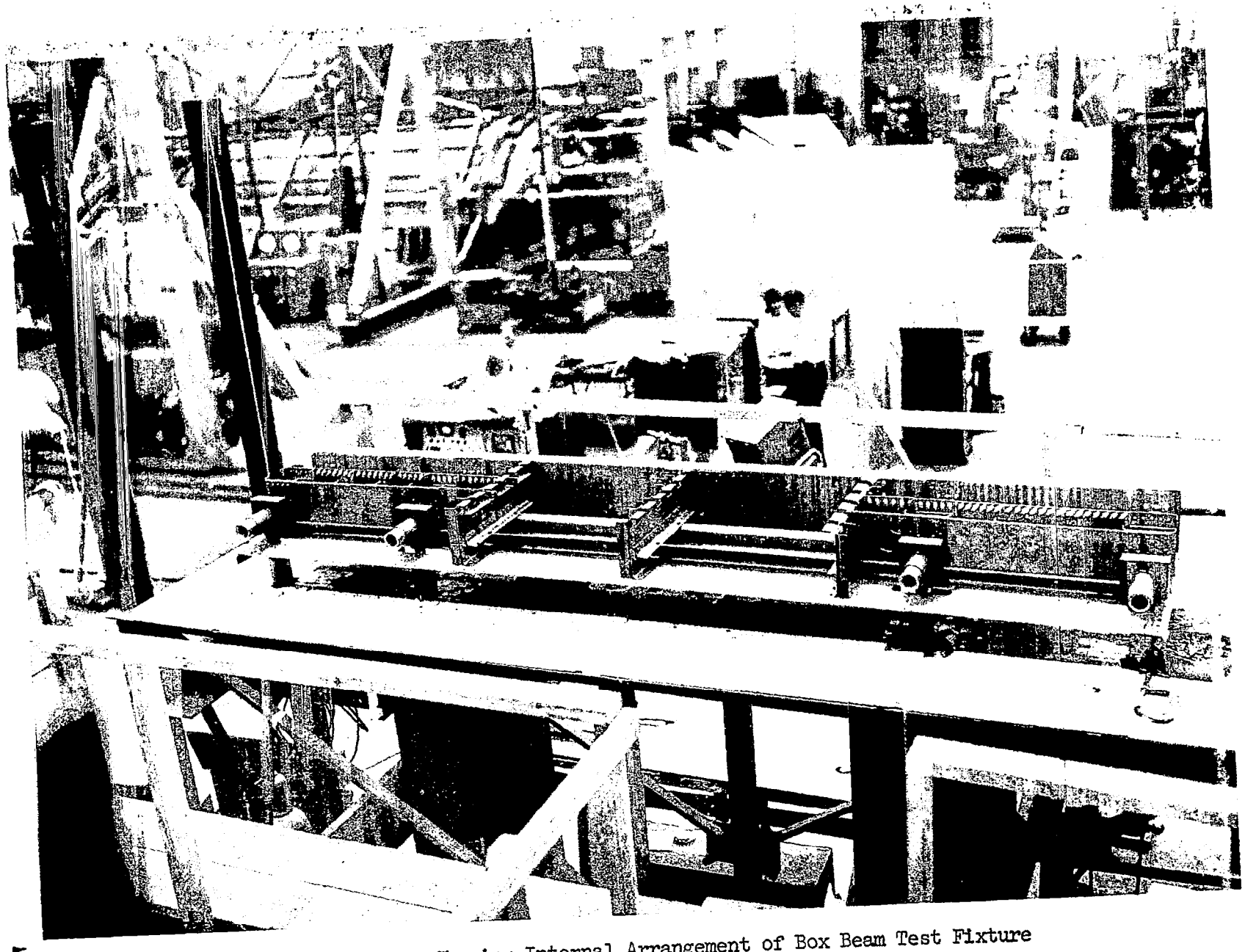

Figure 7. View Showing Internal Arrangement of Box Beam Test Fixture

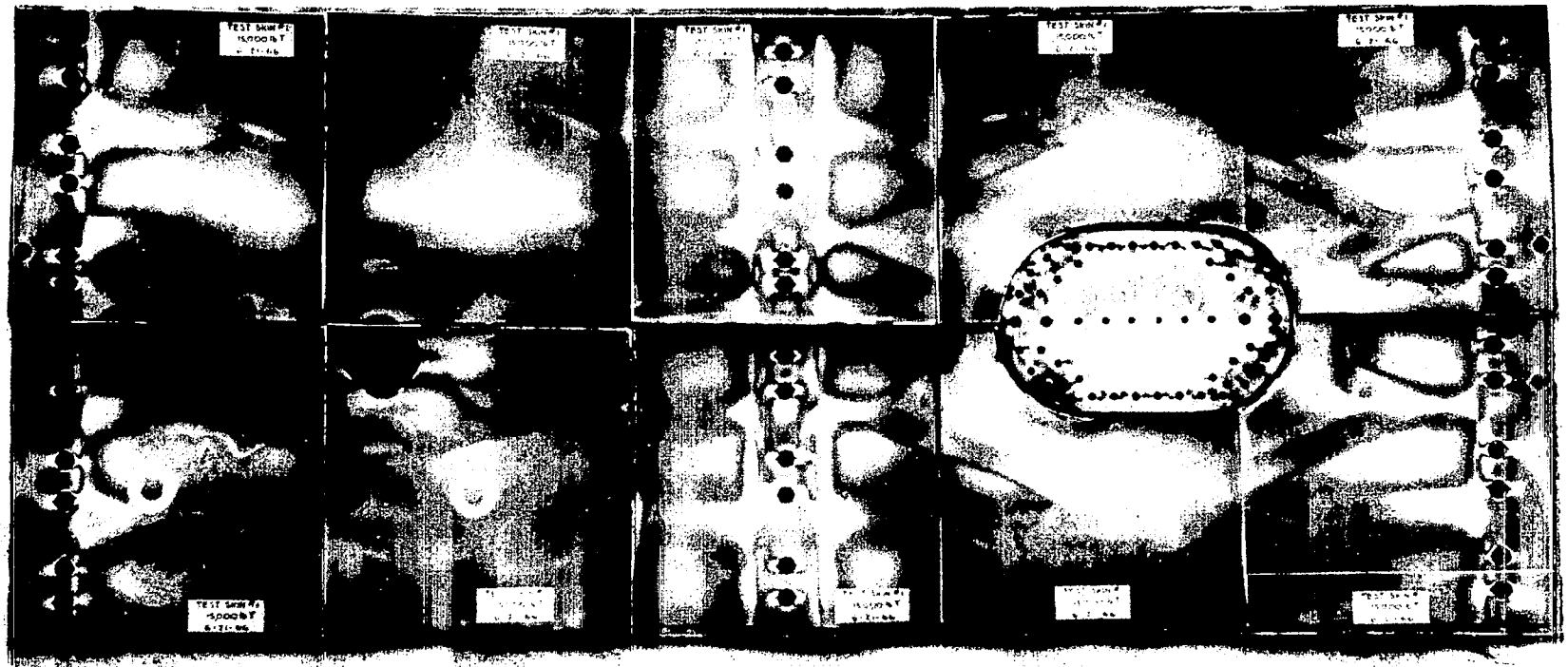

Figure 8. Composite Photograph Showing Isochromatics at Applied Load of 15,000 Pounds

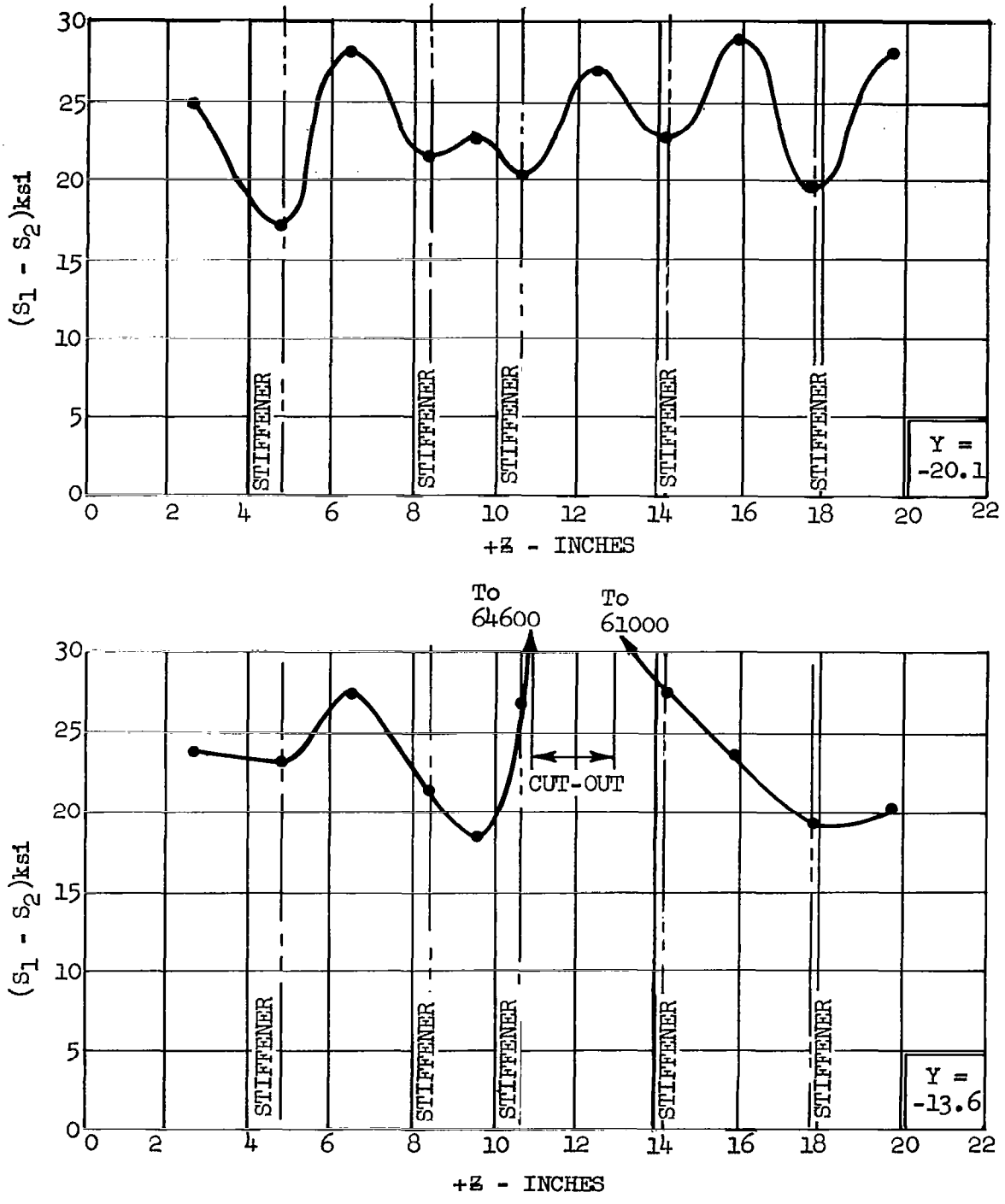

Figure 9. Sketch Showing Chordwise Values from Photoelastic Readings at Selected Locations for P = 20,000 Pounds

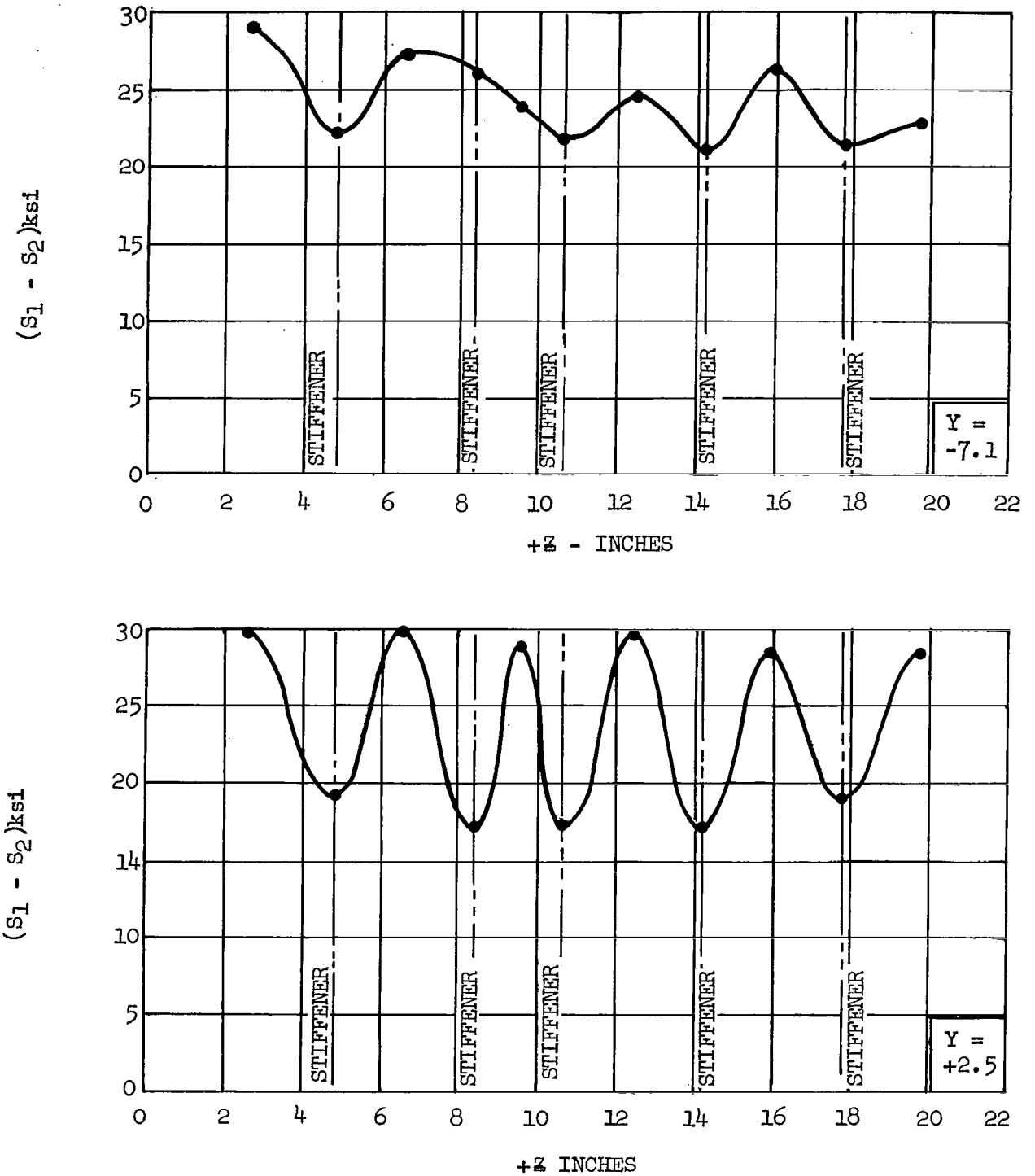

Figure 9. Sketch Showing Chordwise Values from Photoelastic Readings at Selected Locations for P = 20,000 Pounds (Continued)

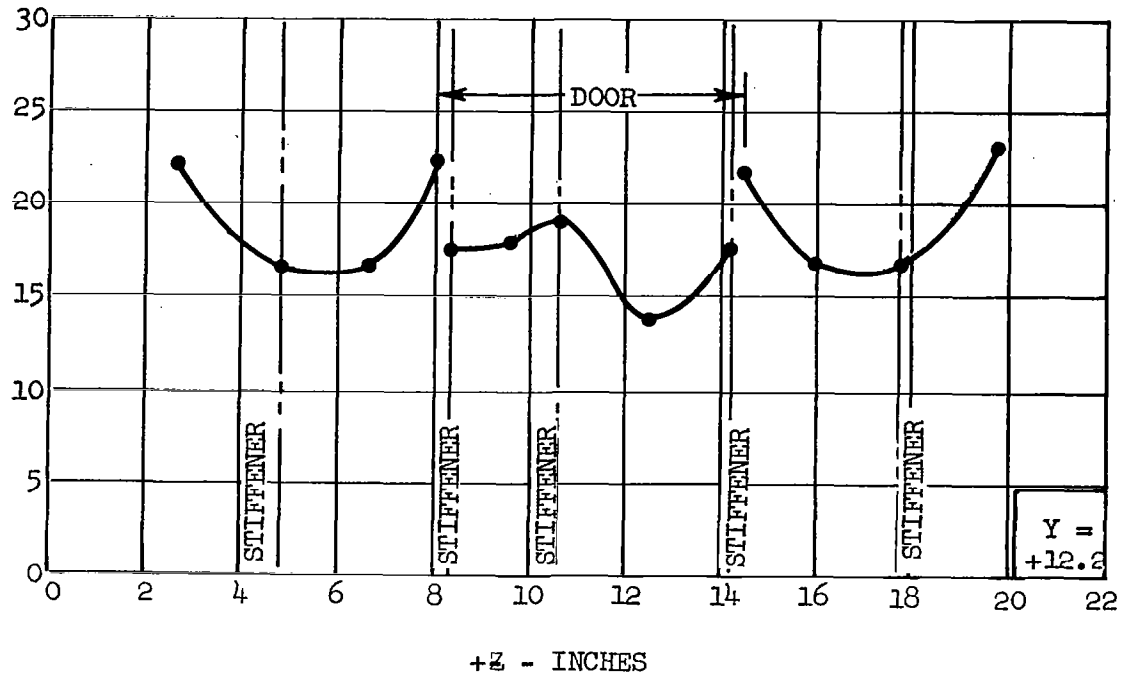

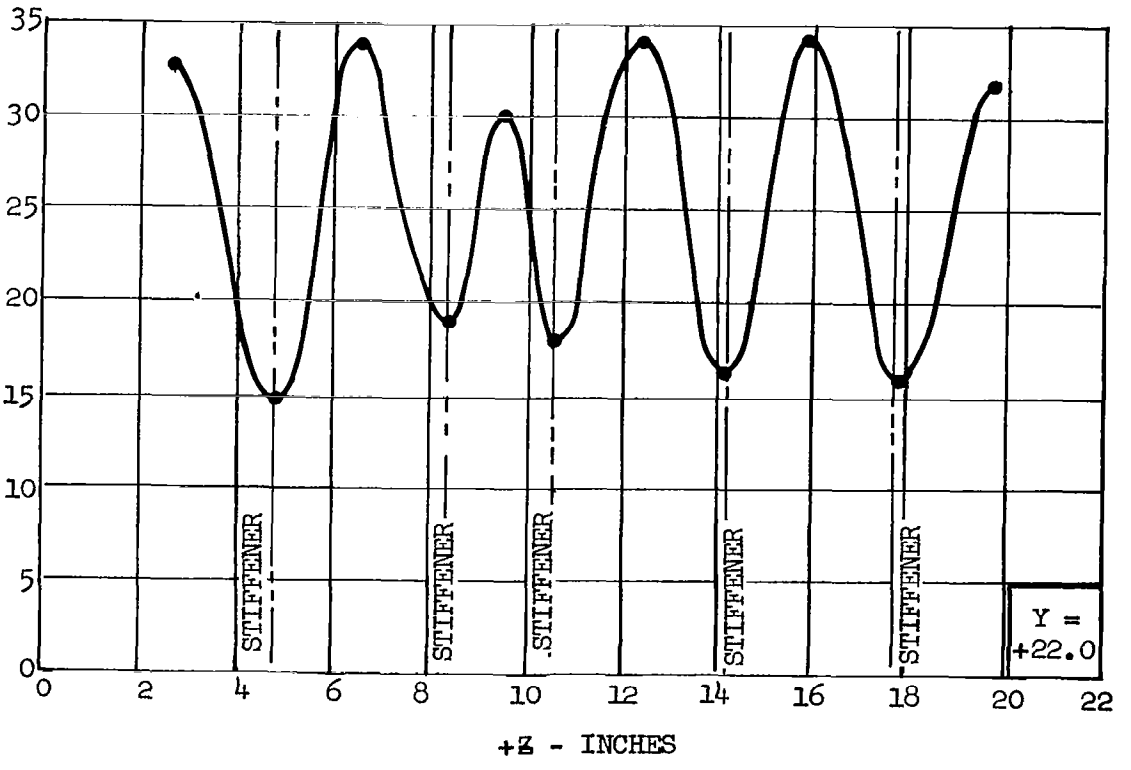

Figure 9. Sketch Showing Chordwise Values from Photoelastic Readings at Selected Locations for P = 20,000 Pounds (Concluded)

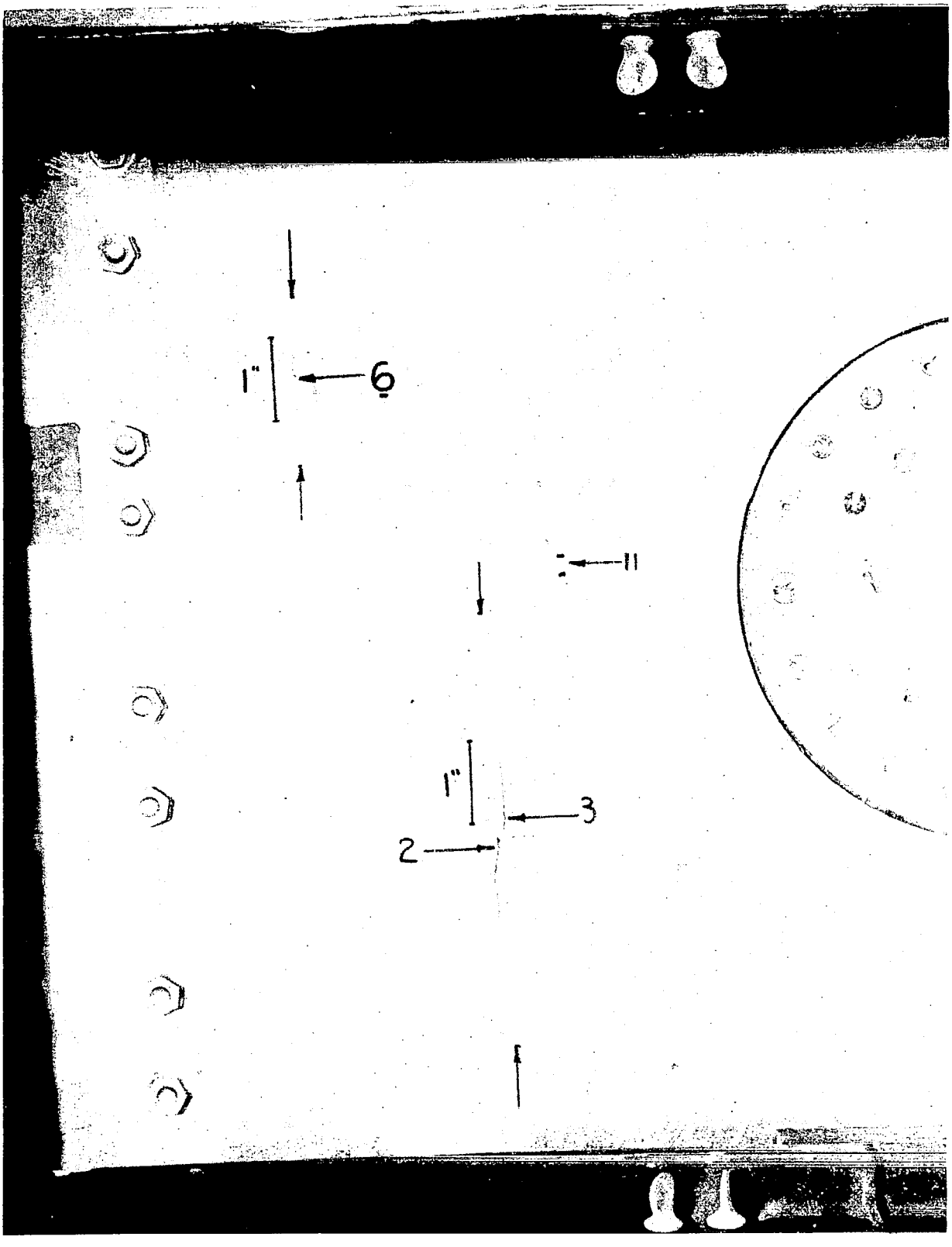

Figure 10. Photograph Showing Cracks 2, 3, and 6, Specimen No. 1

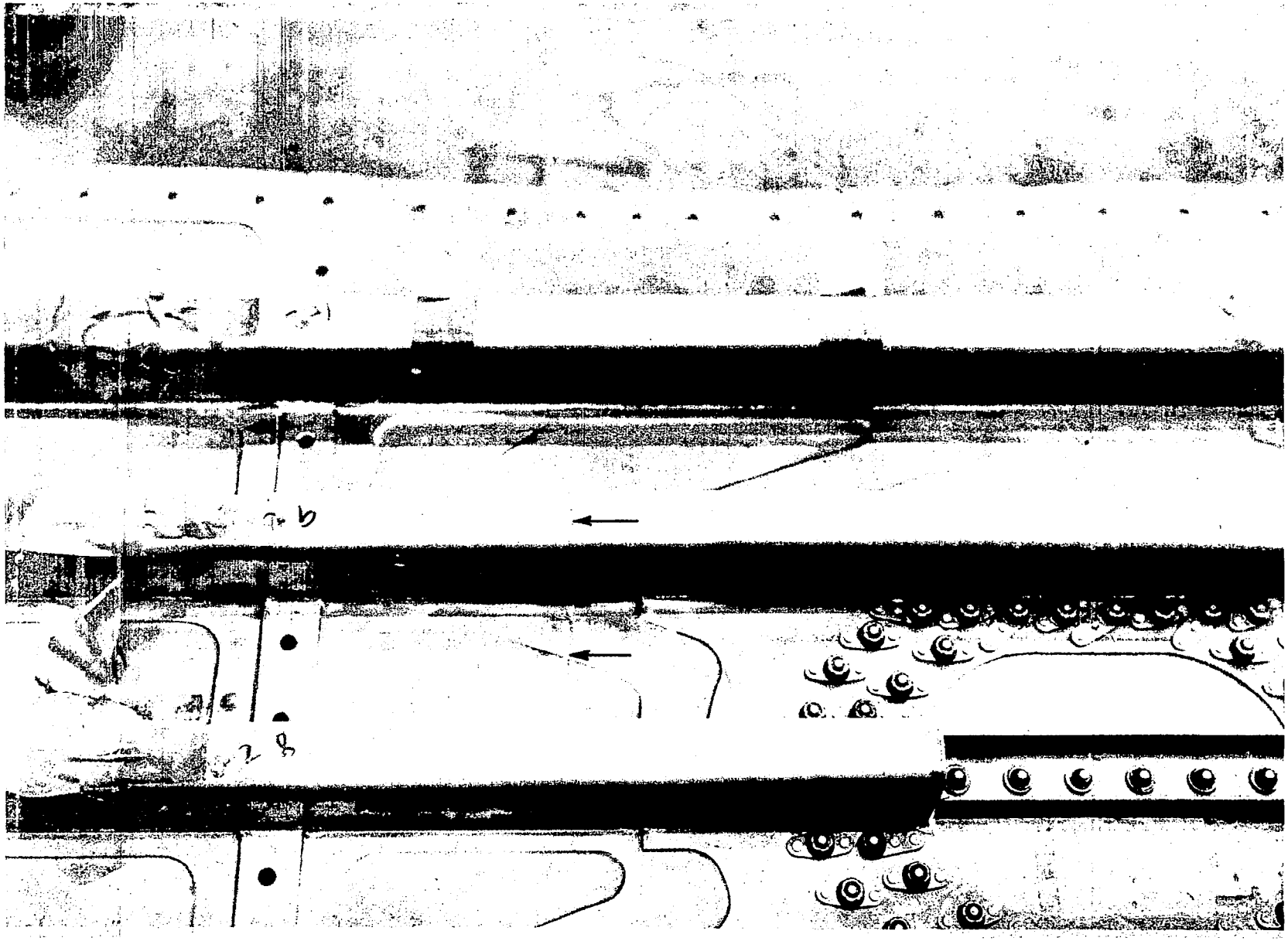

Figure 11. Internal View of Specimen No. 1 Showing Severed Stiffener at Crack No. 2

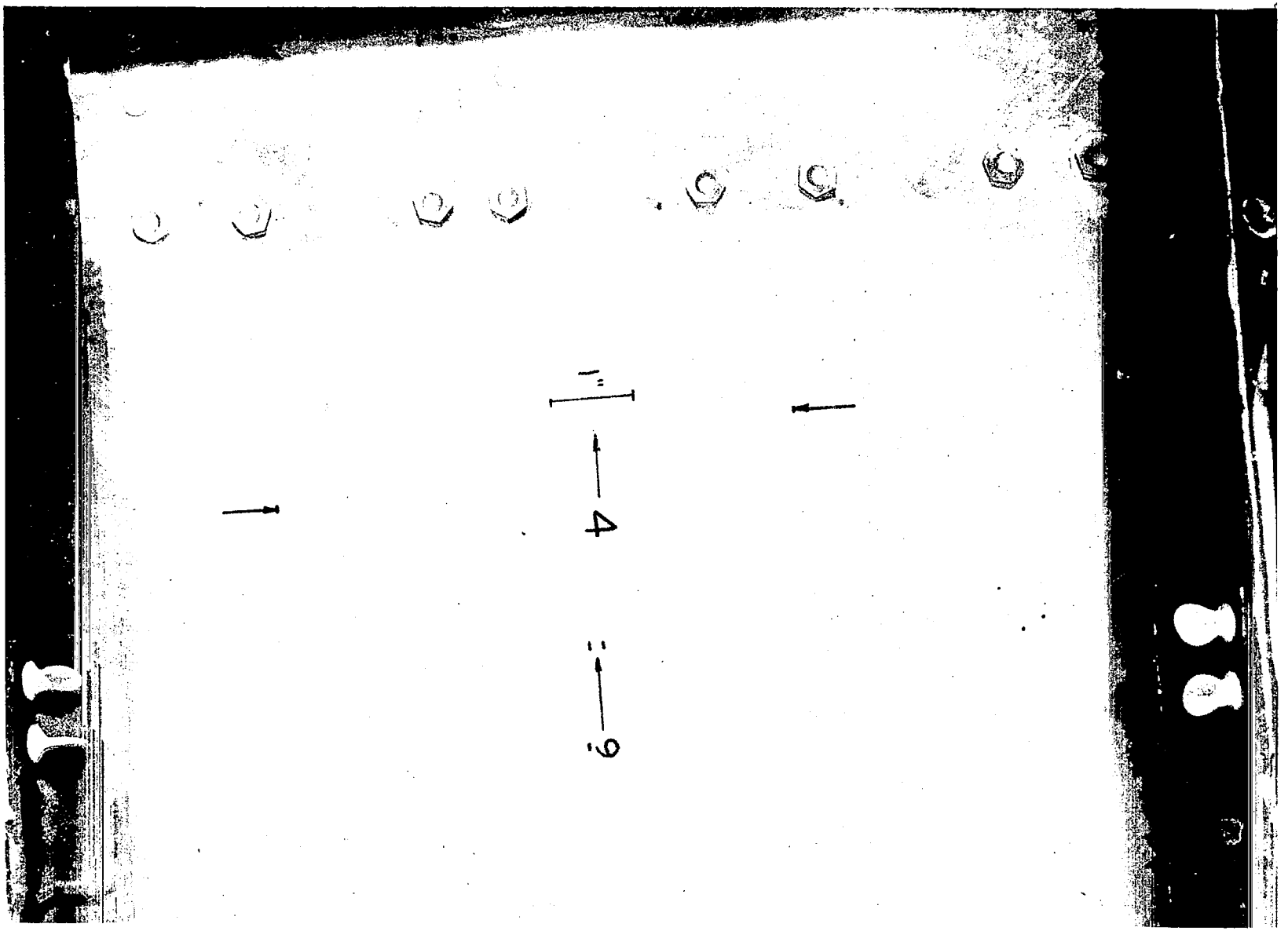

Figure 12. Photograph Showing Crack No. 4, Specimen No. 1

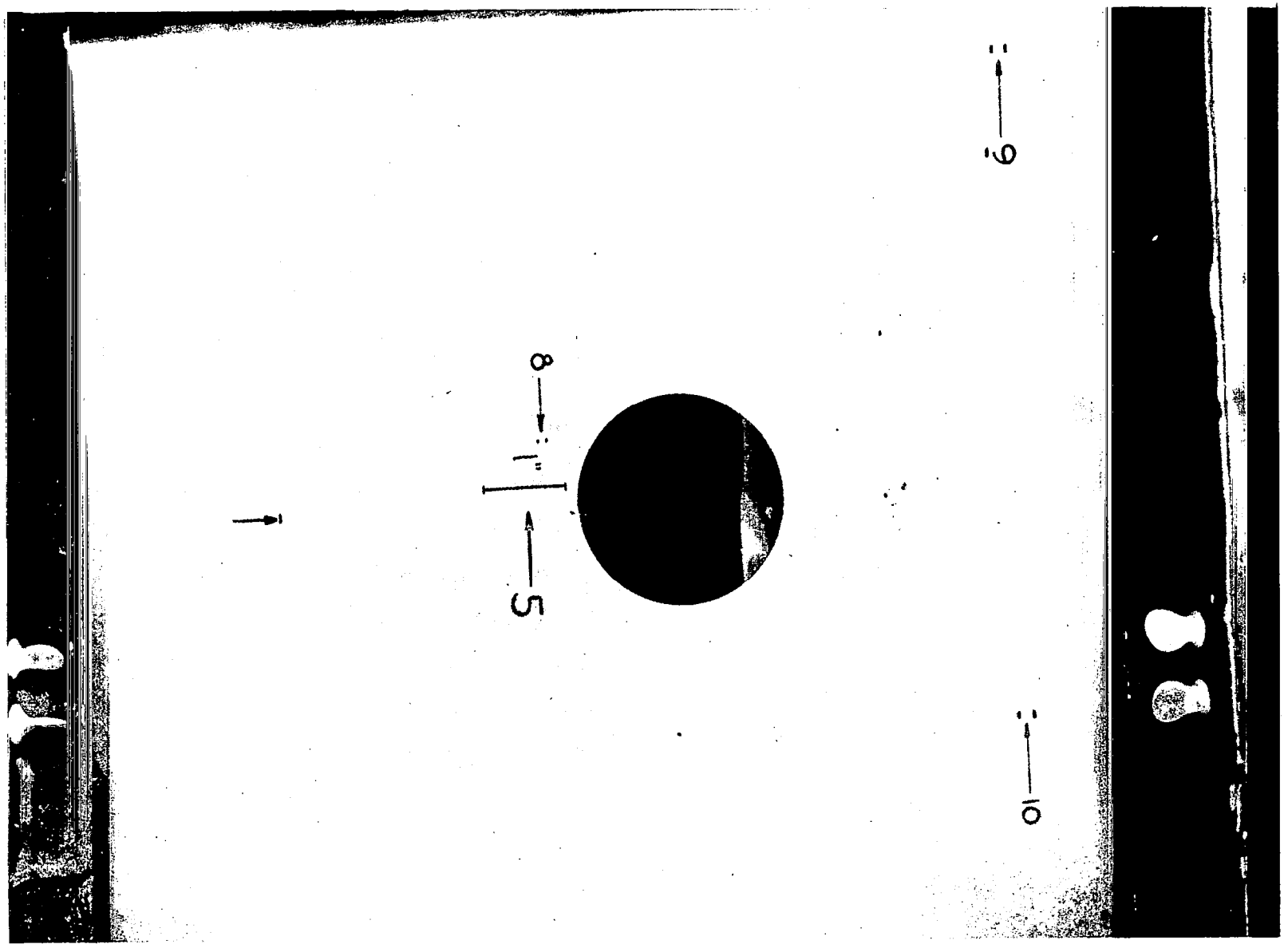

Figure 13. Photograph Showing Crack No. 5, Specimen No. 1

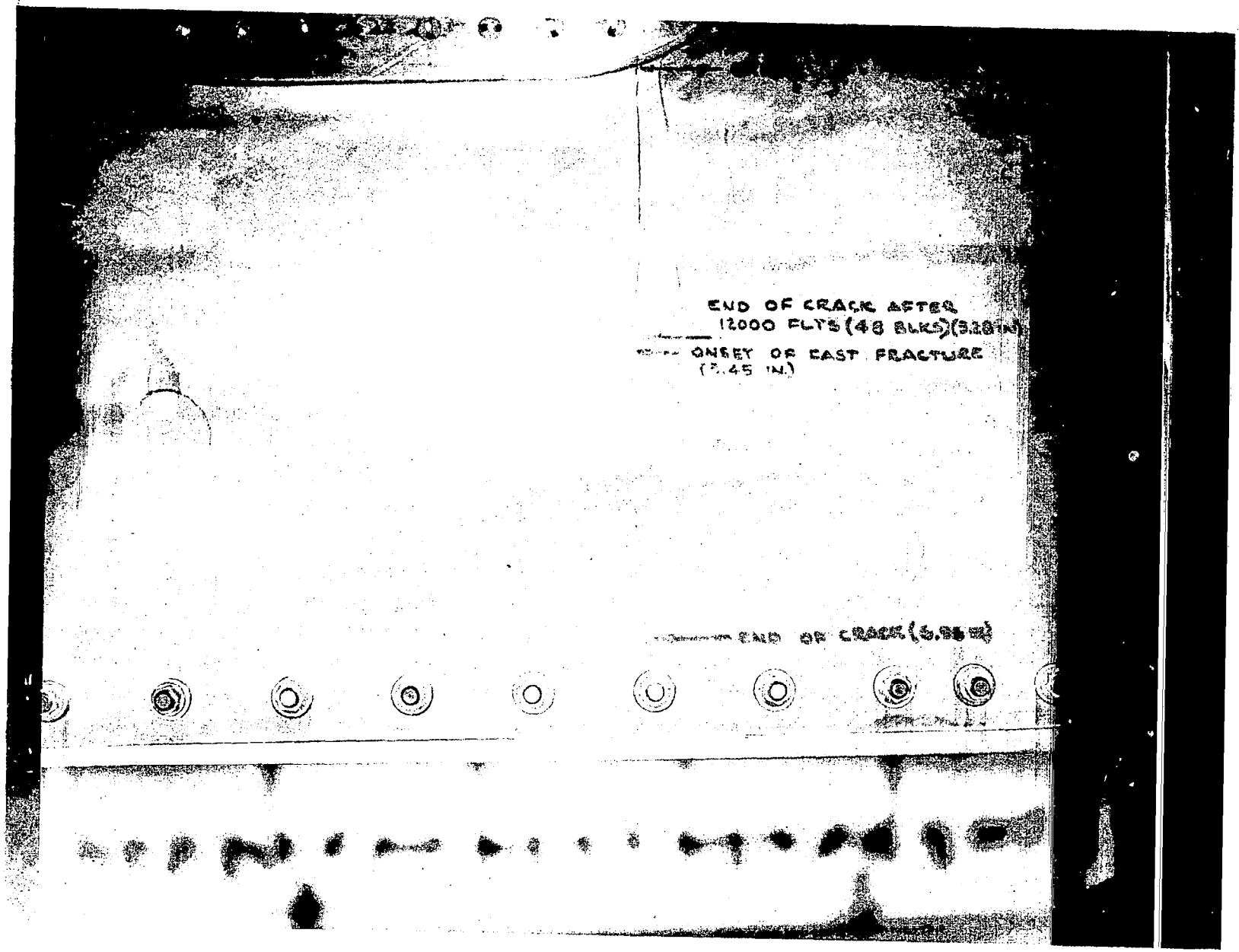

Figure 14. Photograph of Failed Area in Test Specimen No. 4

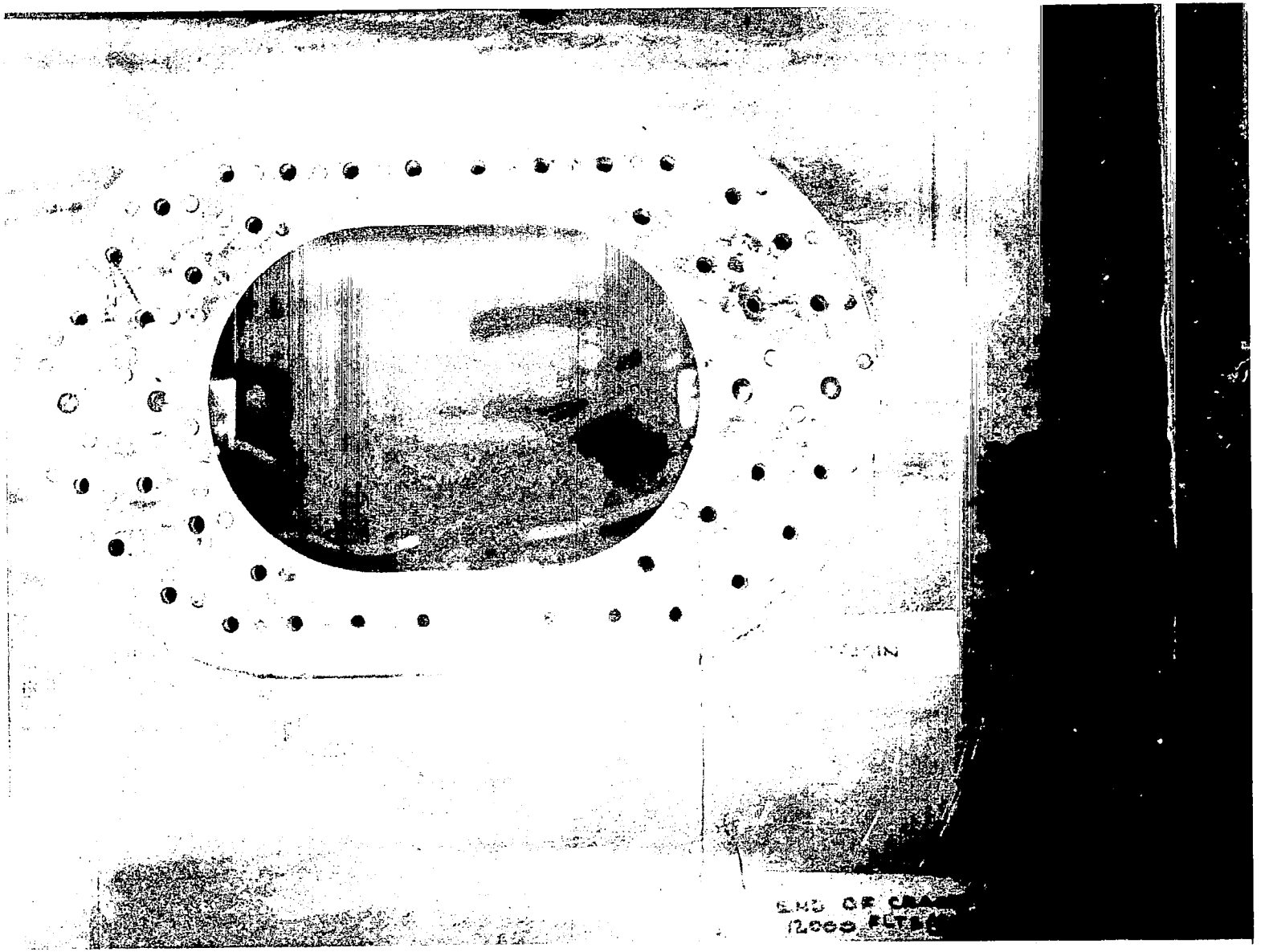

Figure 15. Photograph of Failed Area in Test Specimen No. 4 Showing Extent of Cracking Beneath Door

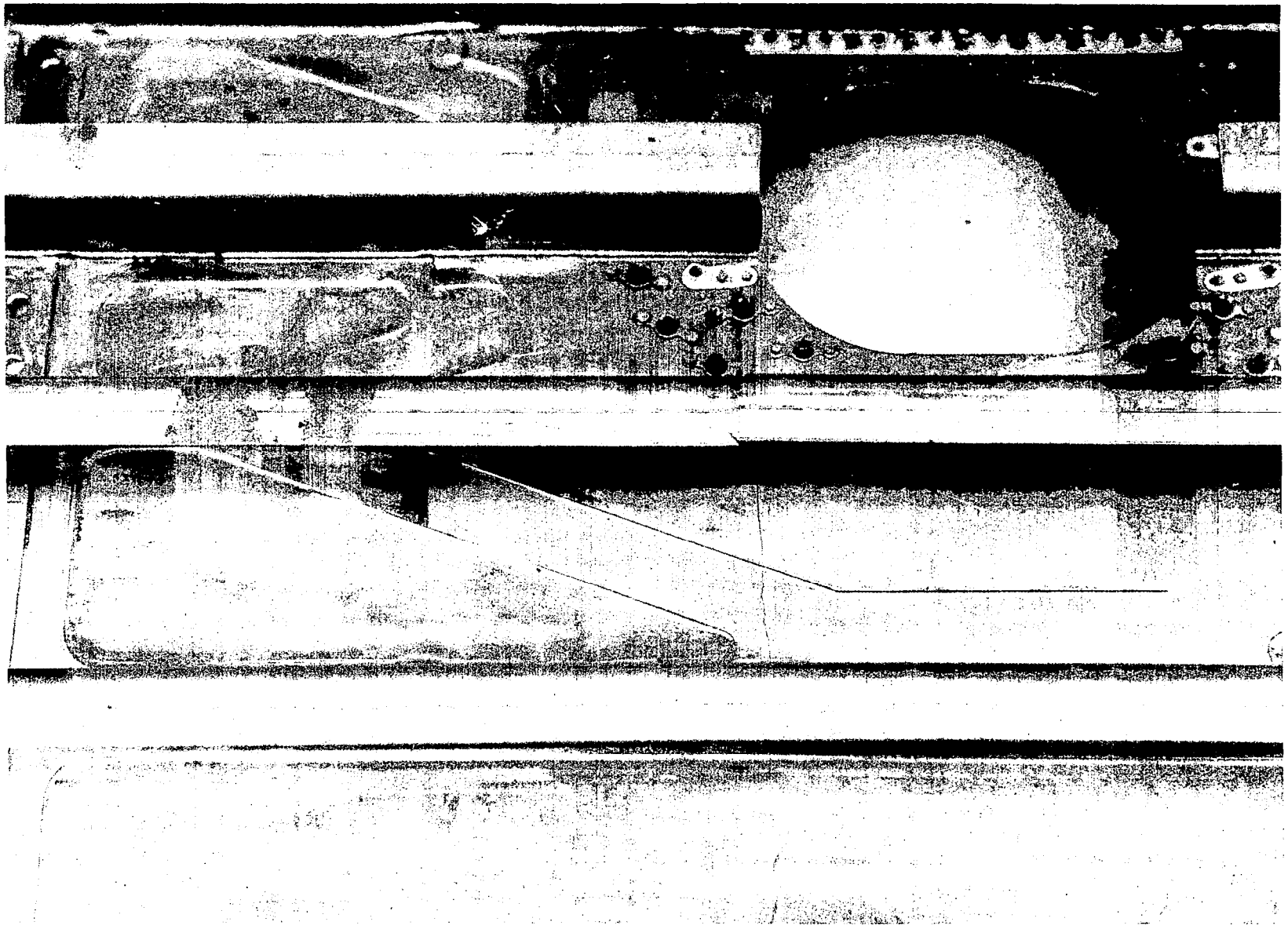

Figure 16. Inside View of Failed Area, Specimen No. 4. Note Failed Stiffener

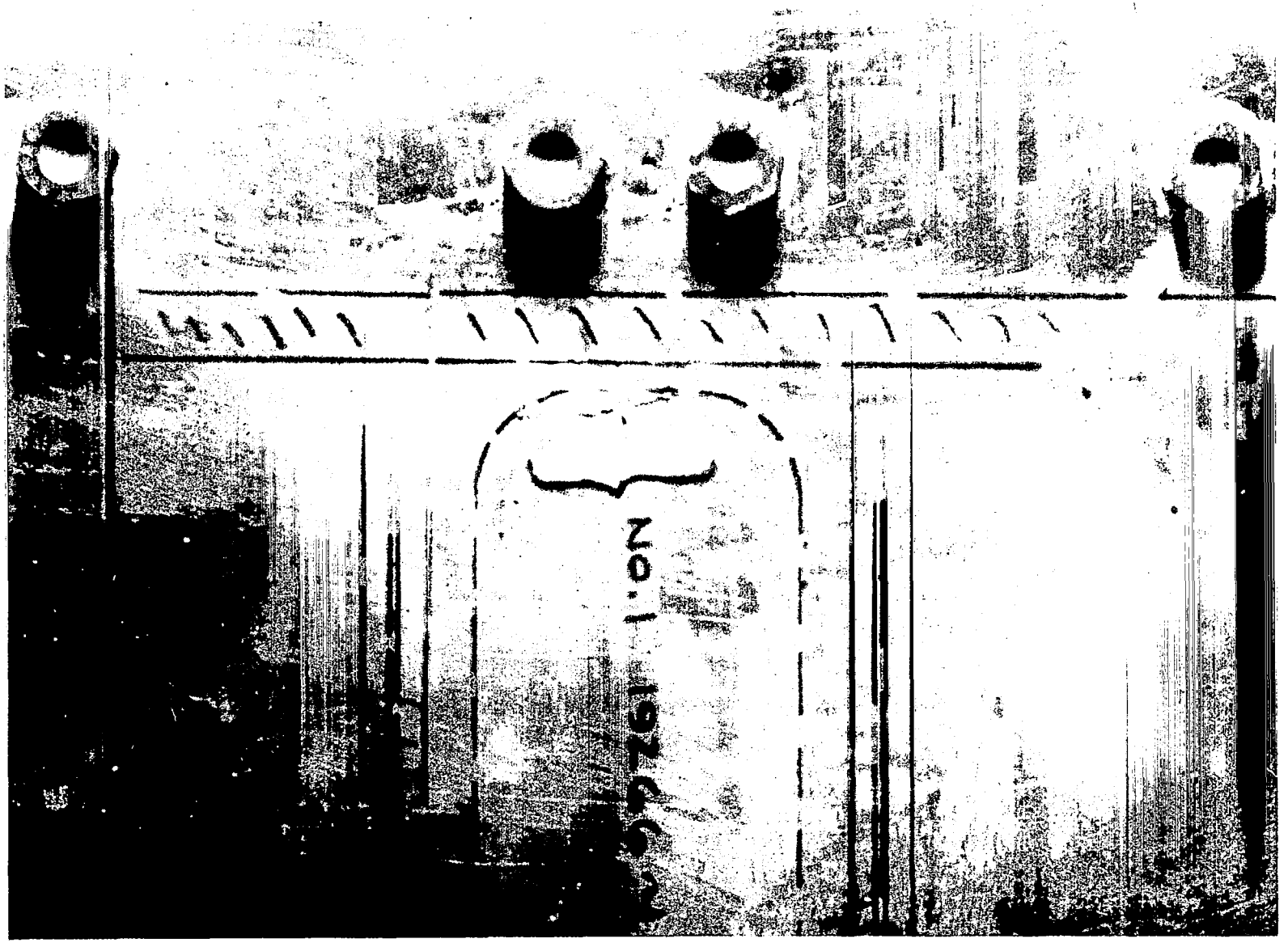

Figure 17. Photograph of Crack No. 1, Specimen No. 1

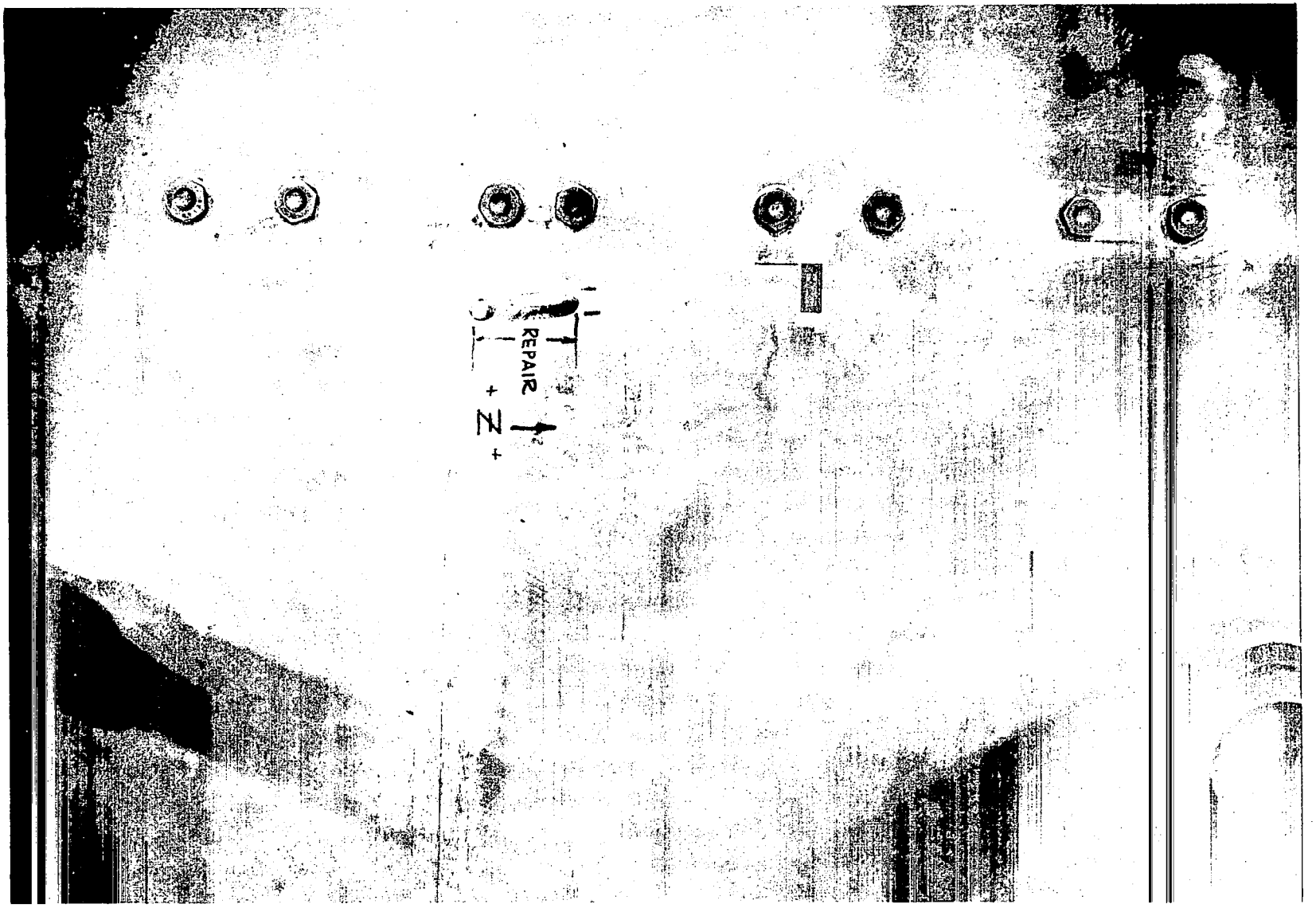

Figure 18. Photograph Showing Repaired Crack in Specimen No. 1 Before Grinding Flush

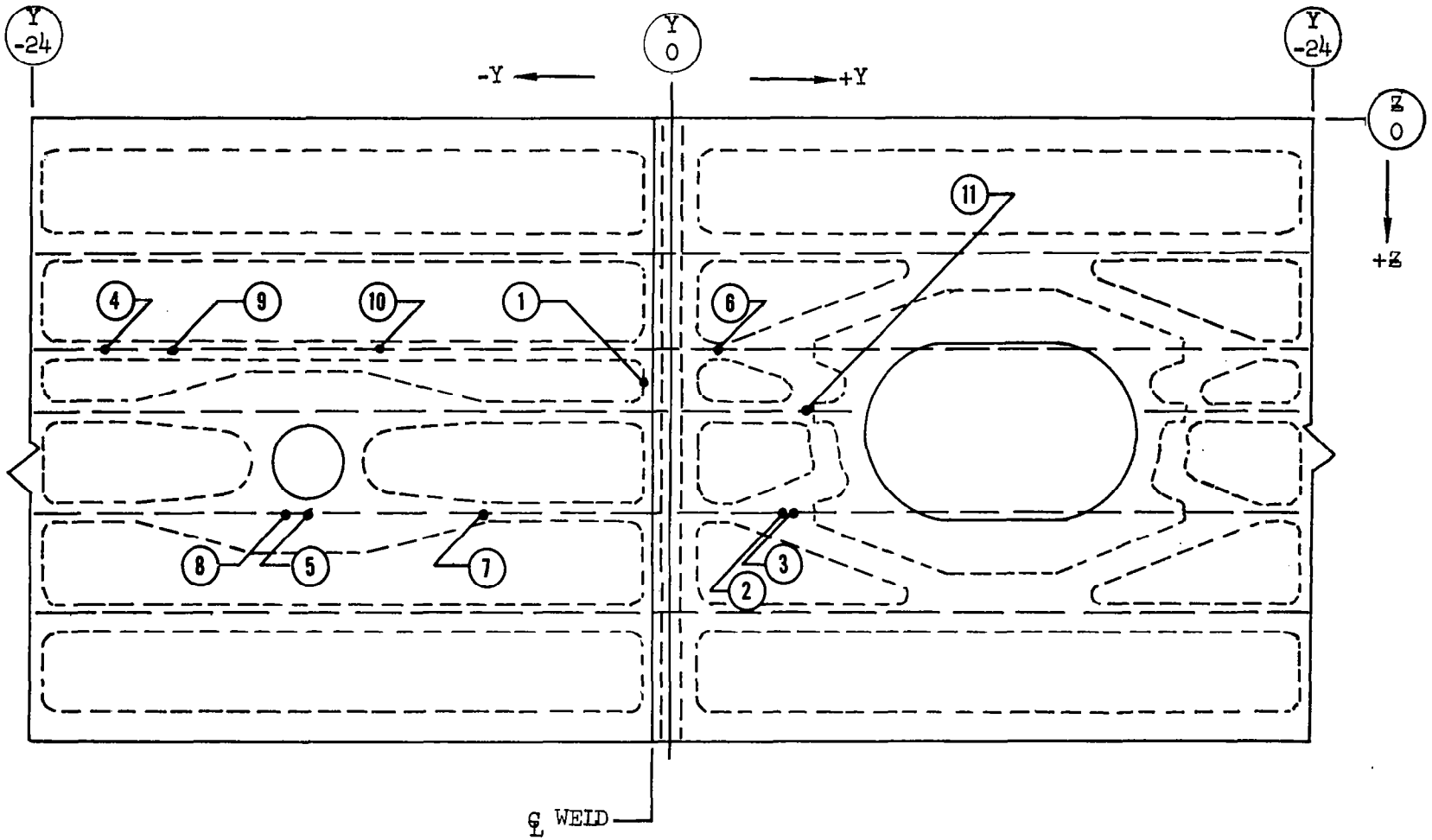

Figure 19. Fatigue Crack Locations in Specimen No. 1

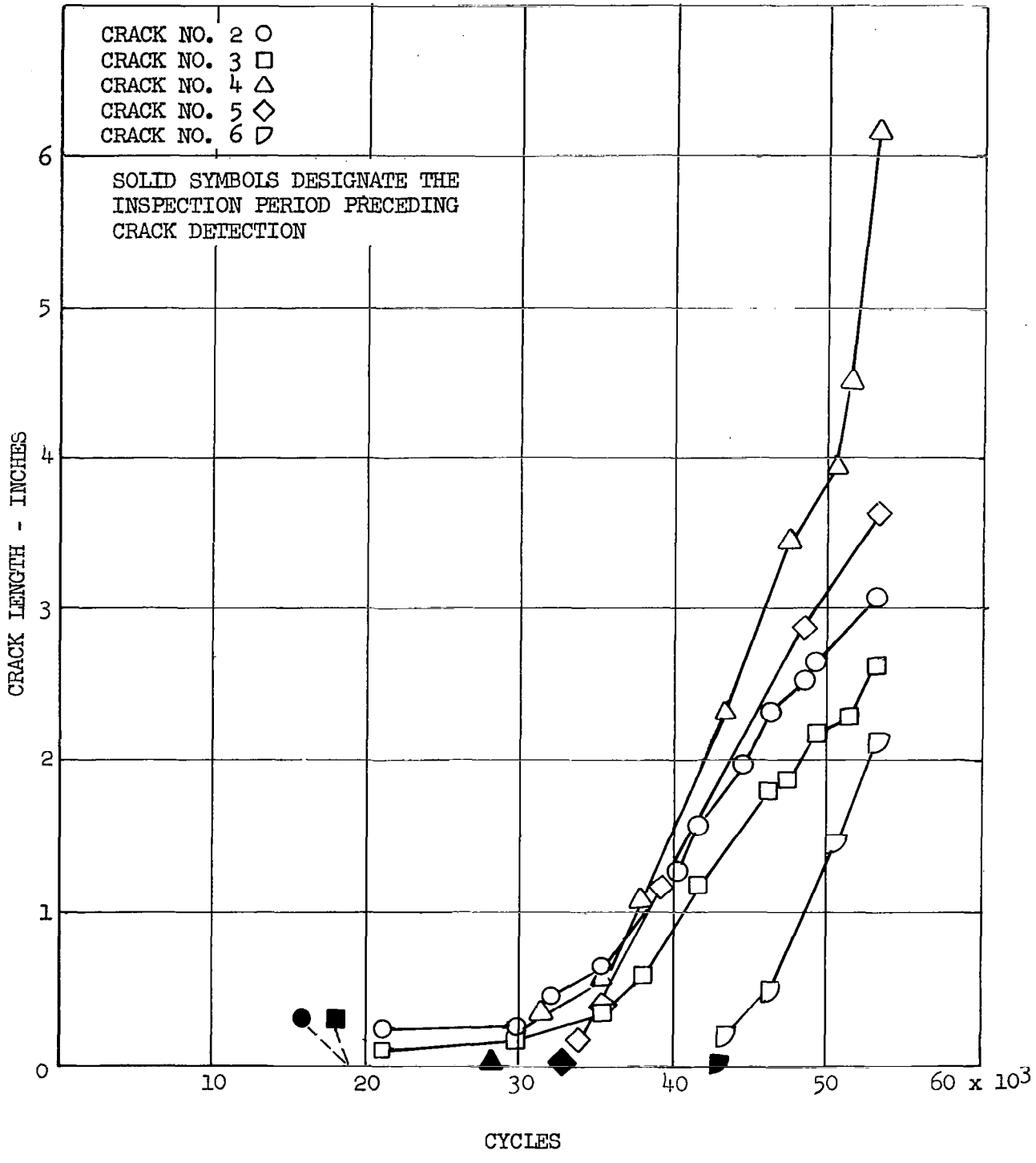

Figure 20. Crack Propagation Curves for Selected Cracks, Test Specimen No. 1

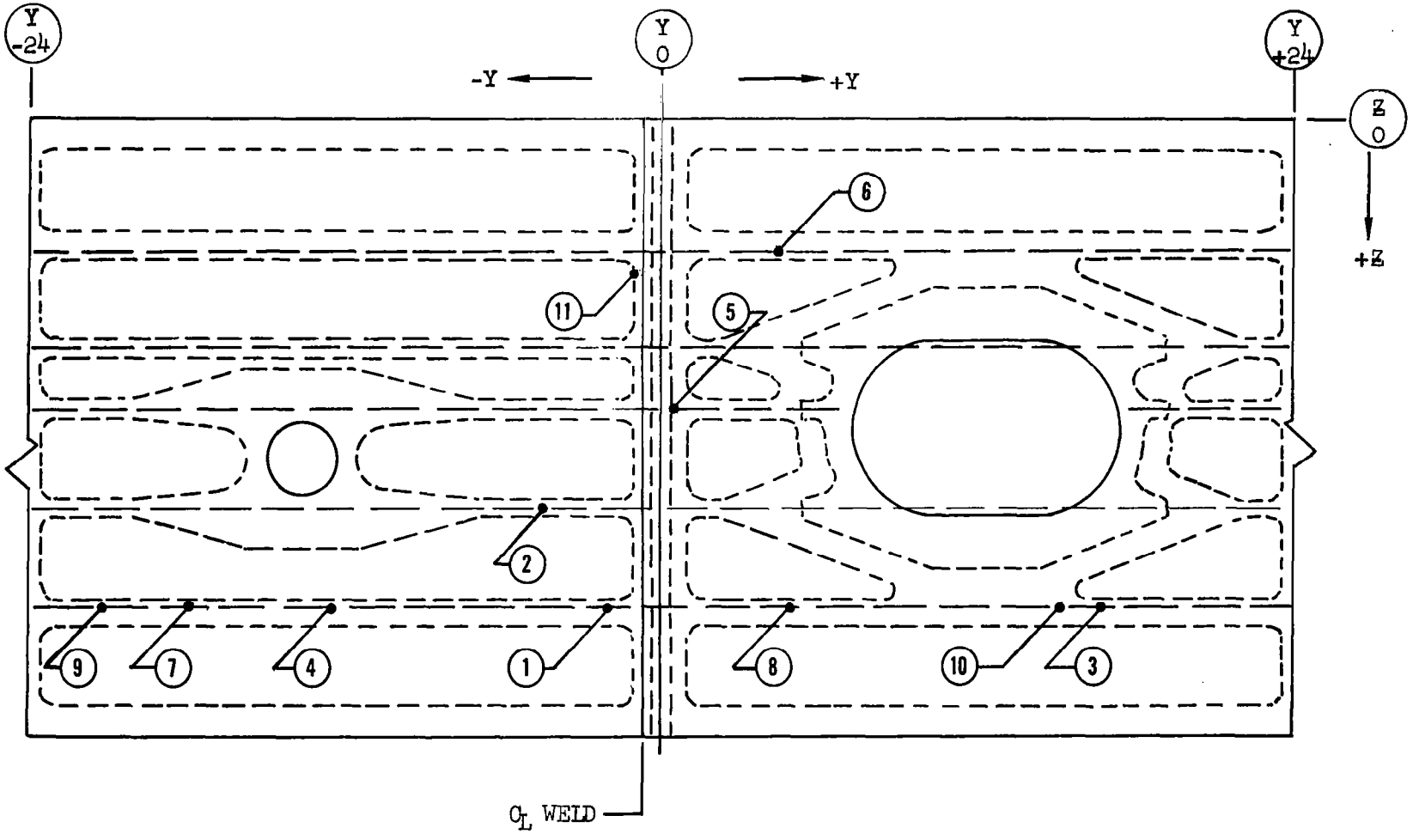

Figure 21. Fatigue Crack Locations in Specimen No. 3

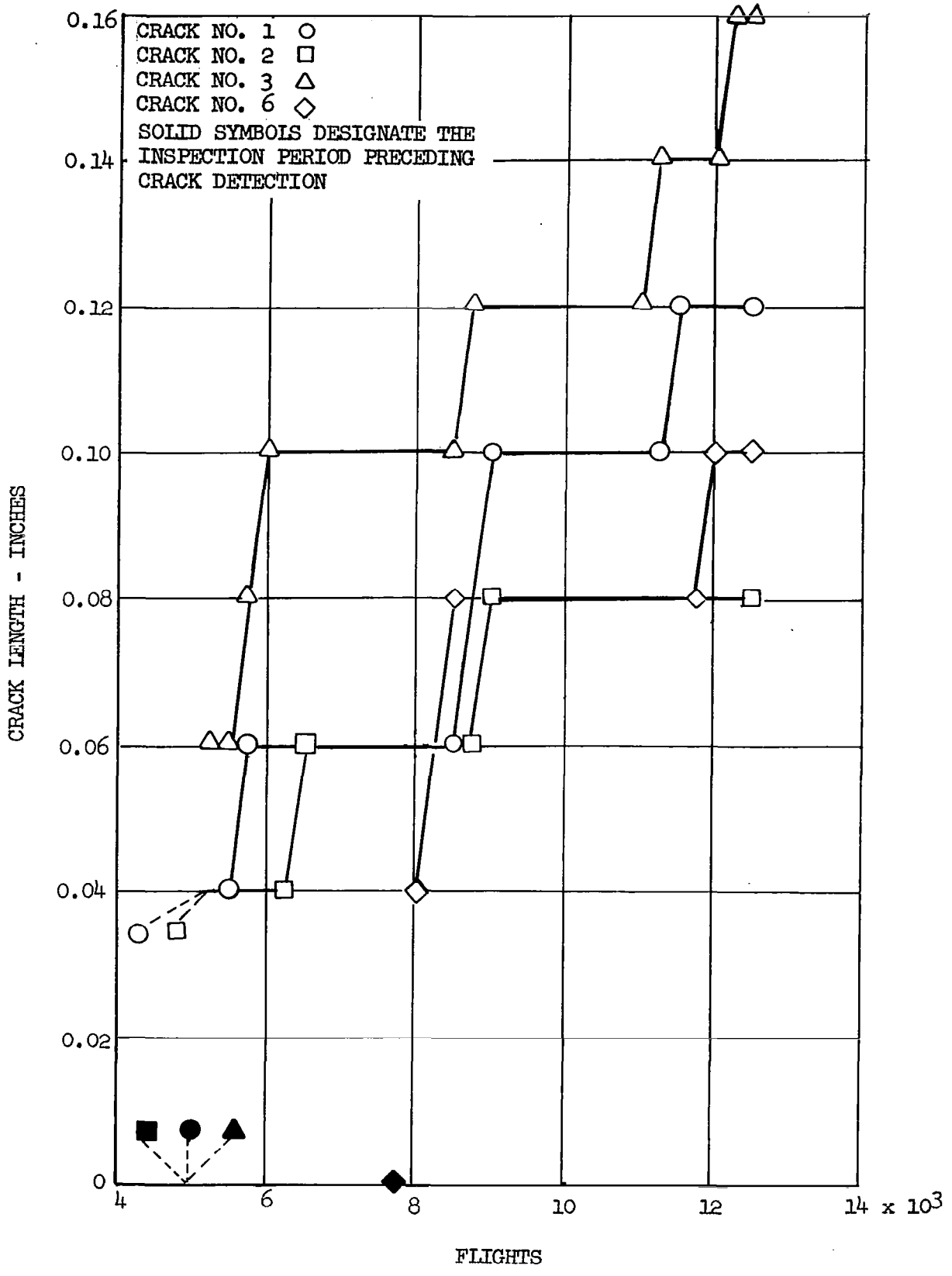

Figure 22. Crack Propagation Curves for Selected Cracks, Test Specimen No. 3

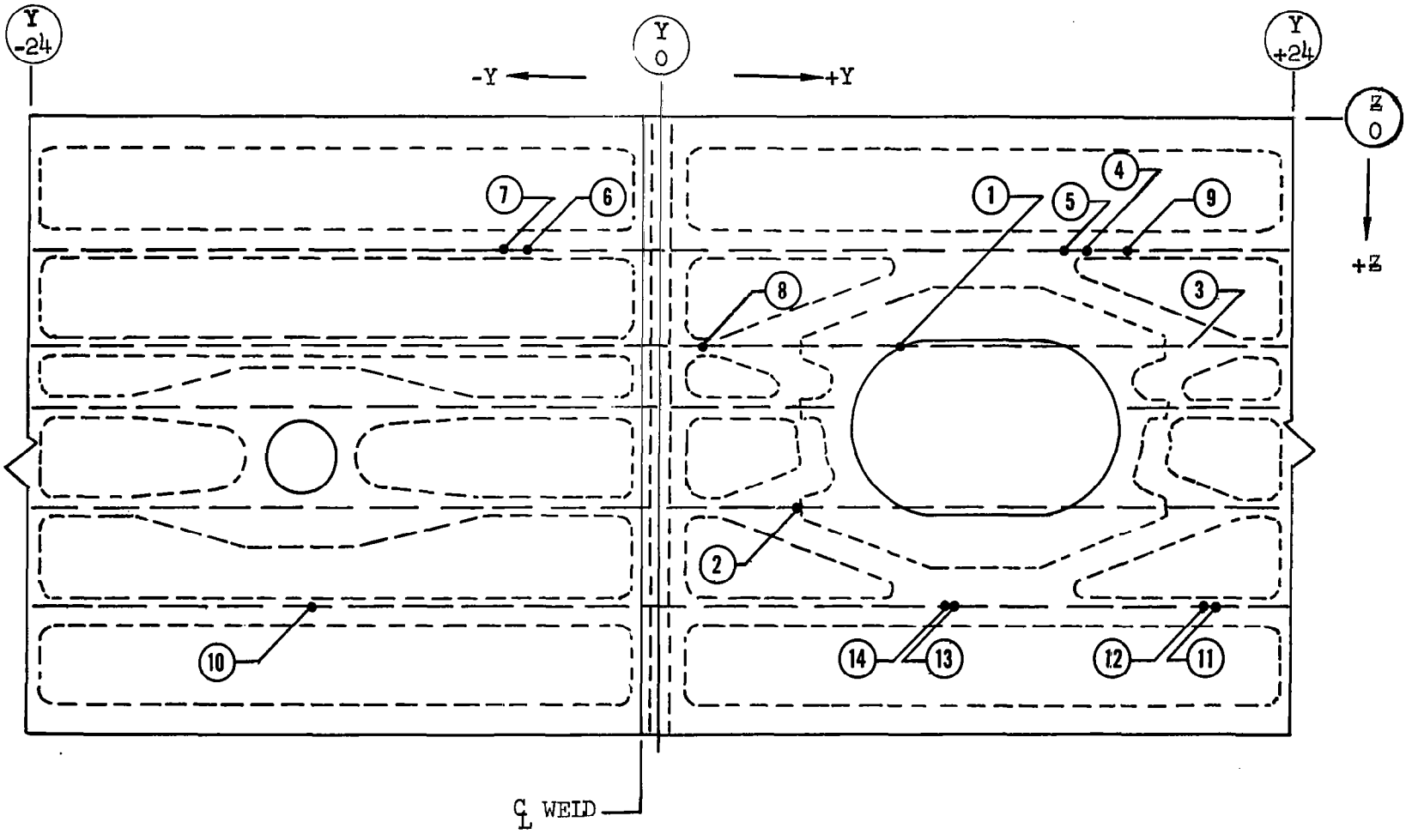

Figure 23. Fatigue Crack Locations in Specimen No. 4

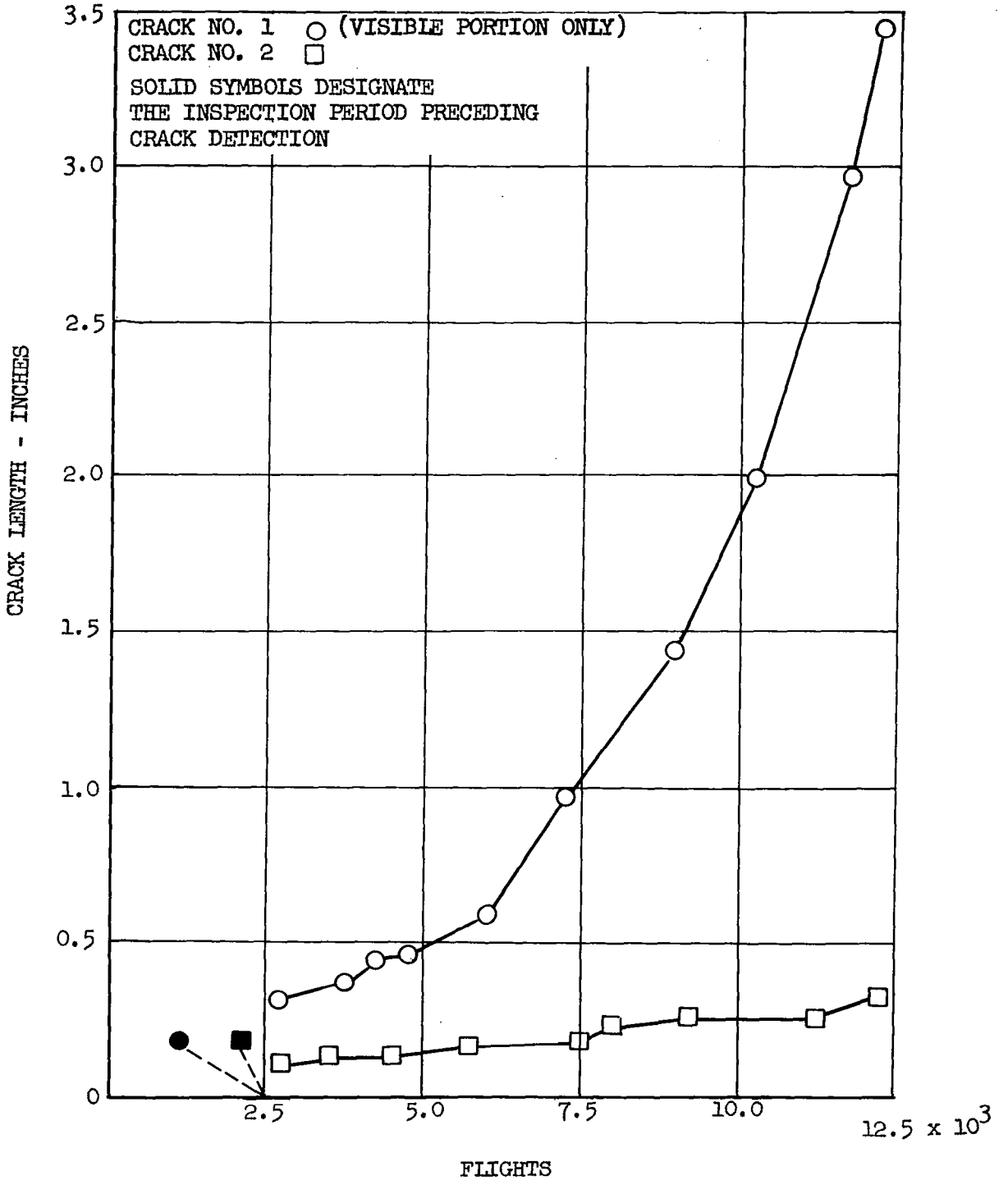

Figure 24. Crack Propagation Curves for Selected Cracks, Test Specimen No. 4

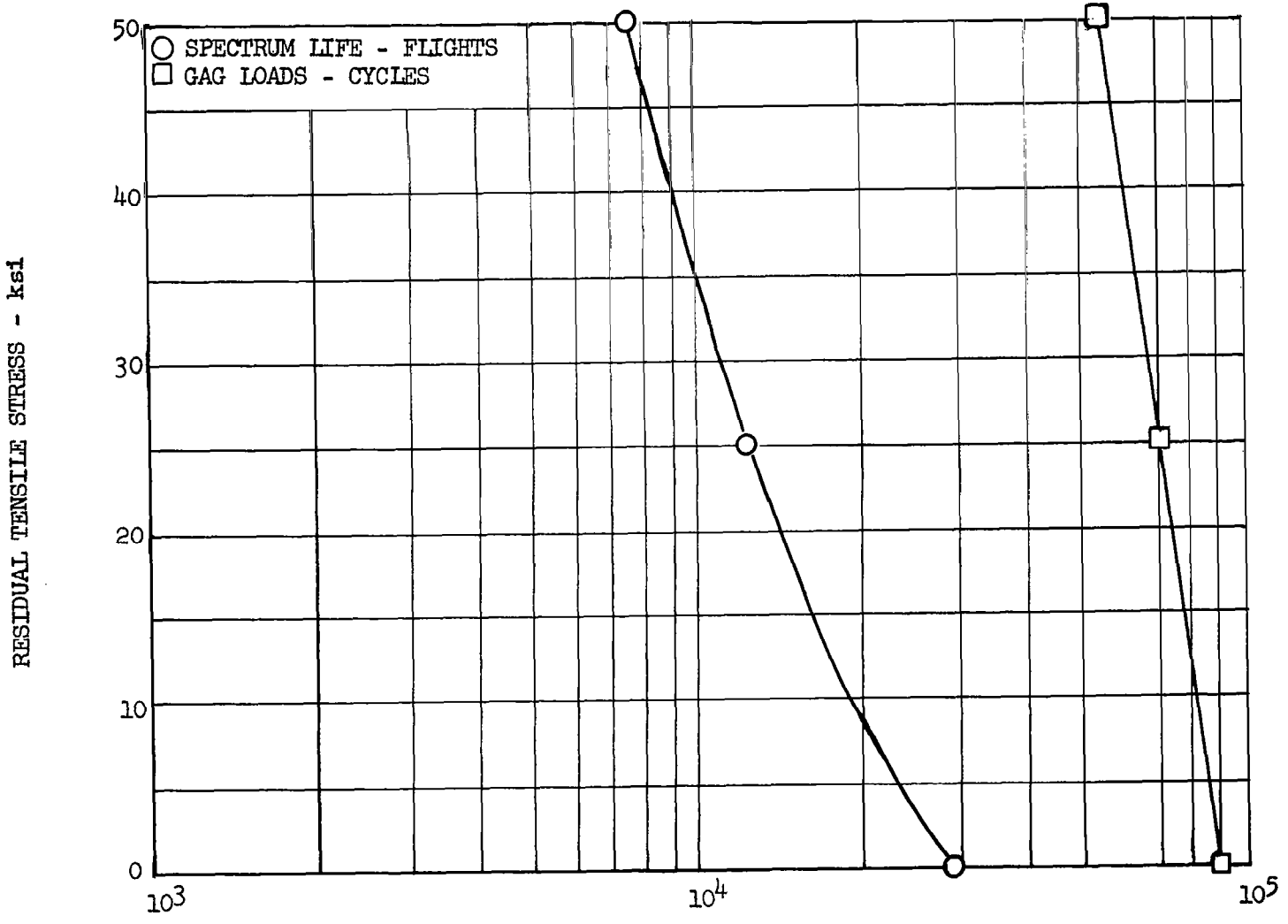

Figure 25. Influence of Residual Stress on Calculated Fatigue Life, $K_T = 4.0$, Reference (3)

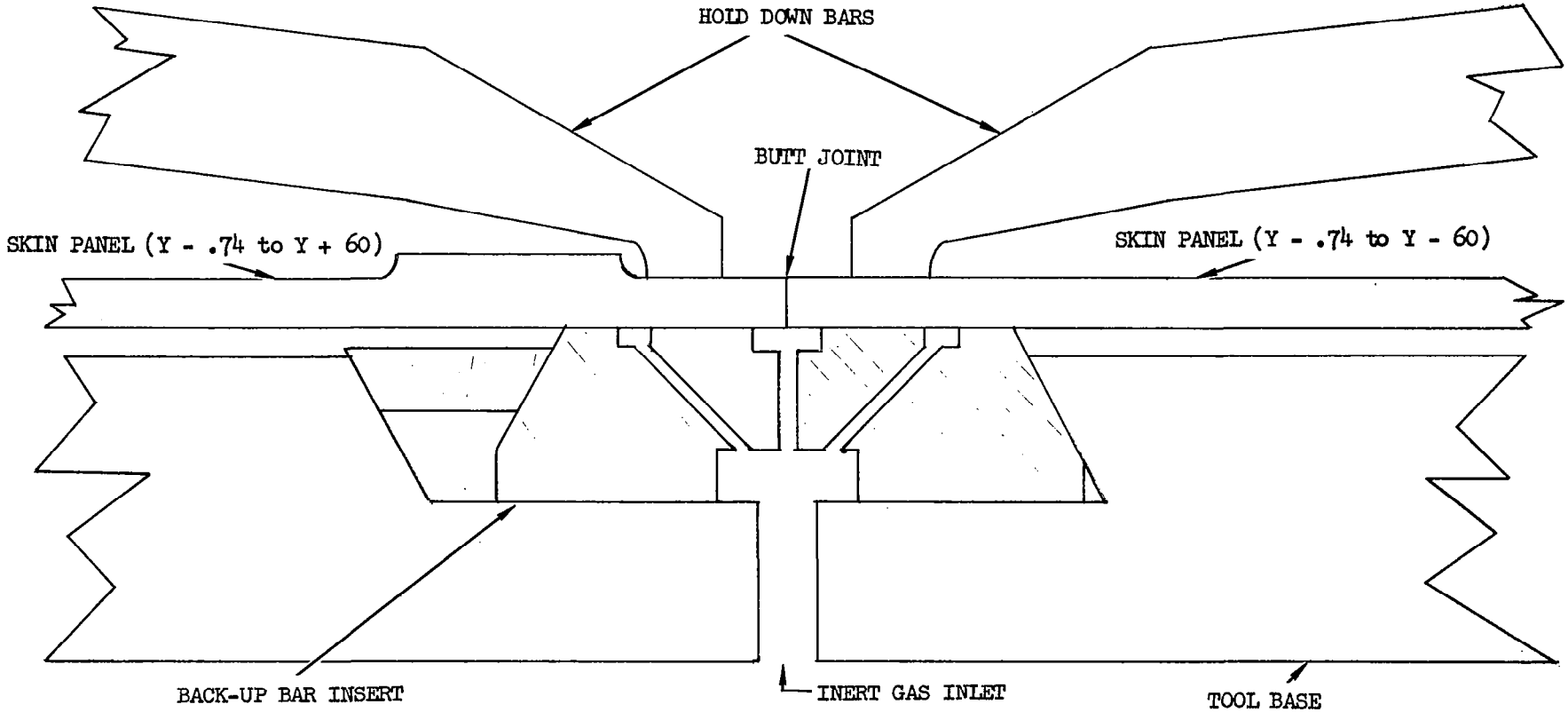

Figure 26. Schematic Drawing of the Fusion Welding Tool for Skin Panel Joining

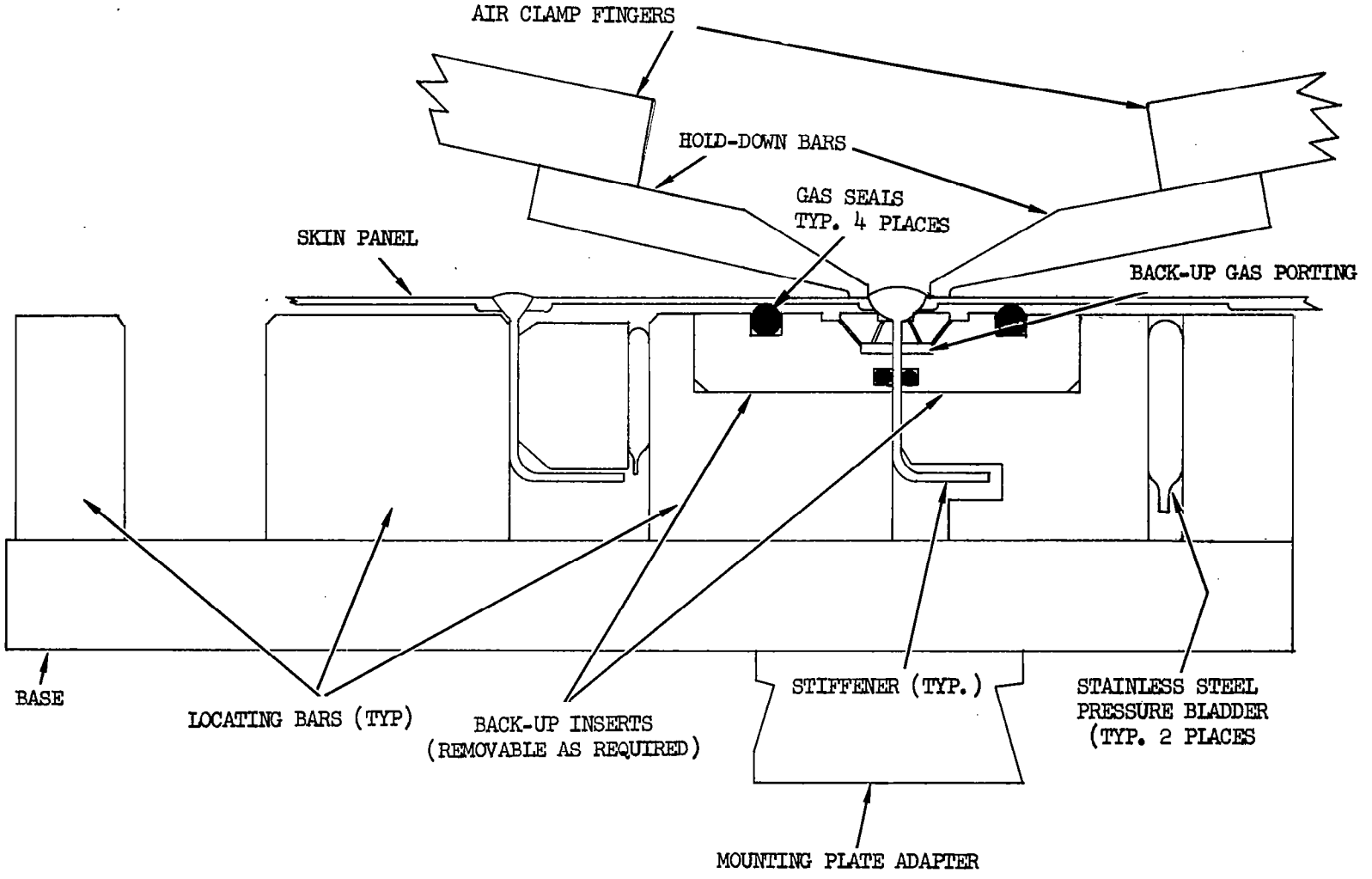

Figure 27. Schematic Drawing of the Stiffener to Skin Fusion Welding Tool

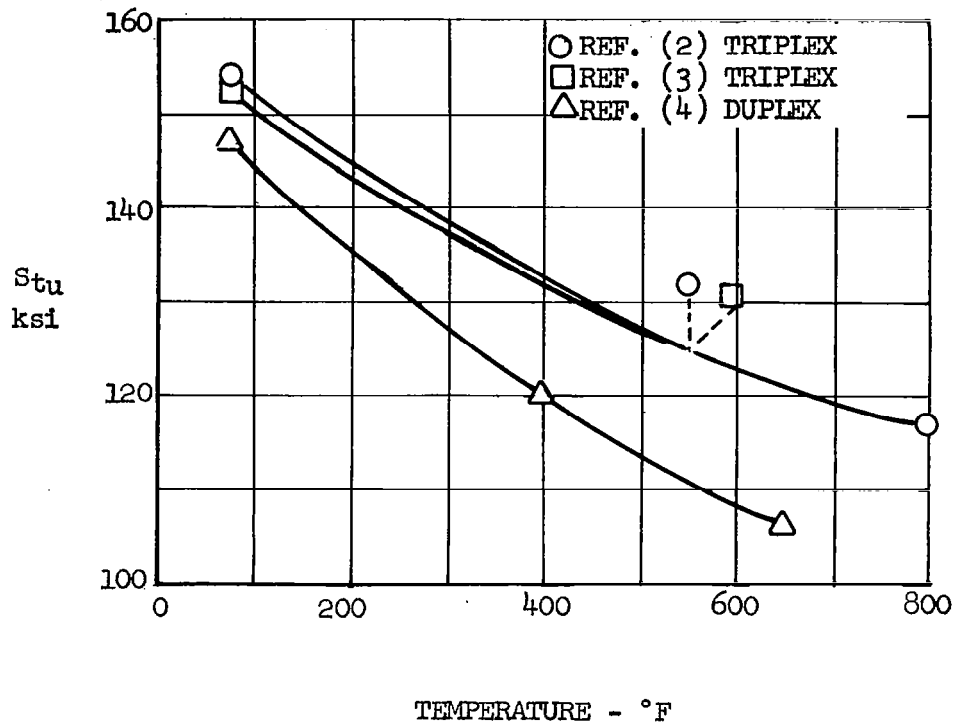

Figure 28. Comparison of Parent Metal Properties, Duplex Annealed and Triplex Annealed Ti-8Al-1Mo-IV

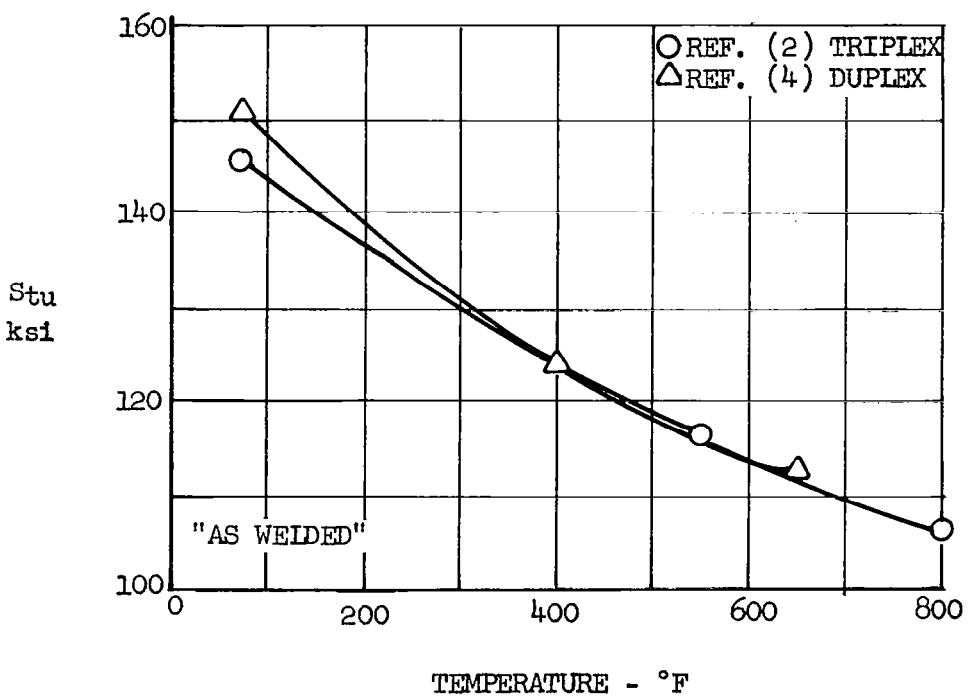

Figure 29. Comparison of Transverse Weld Properties, Duplex Annealed and Triplex Annealed Ti-8Al-1Mo-IV

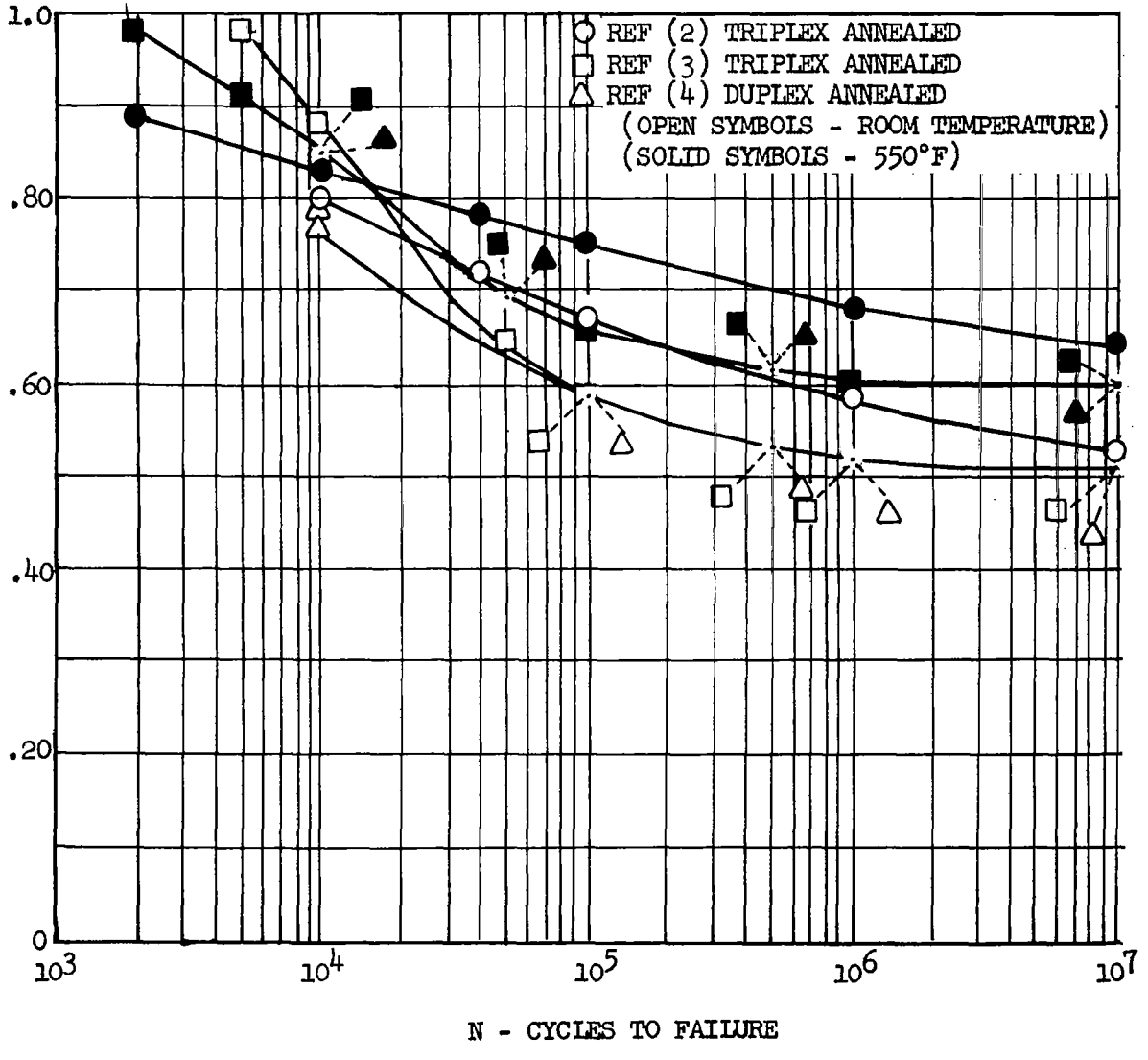

Figure 30. Comparison of Parent Metal Fatigue Life, K_t = 1.0, Smean = 25 ksi

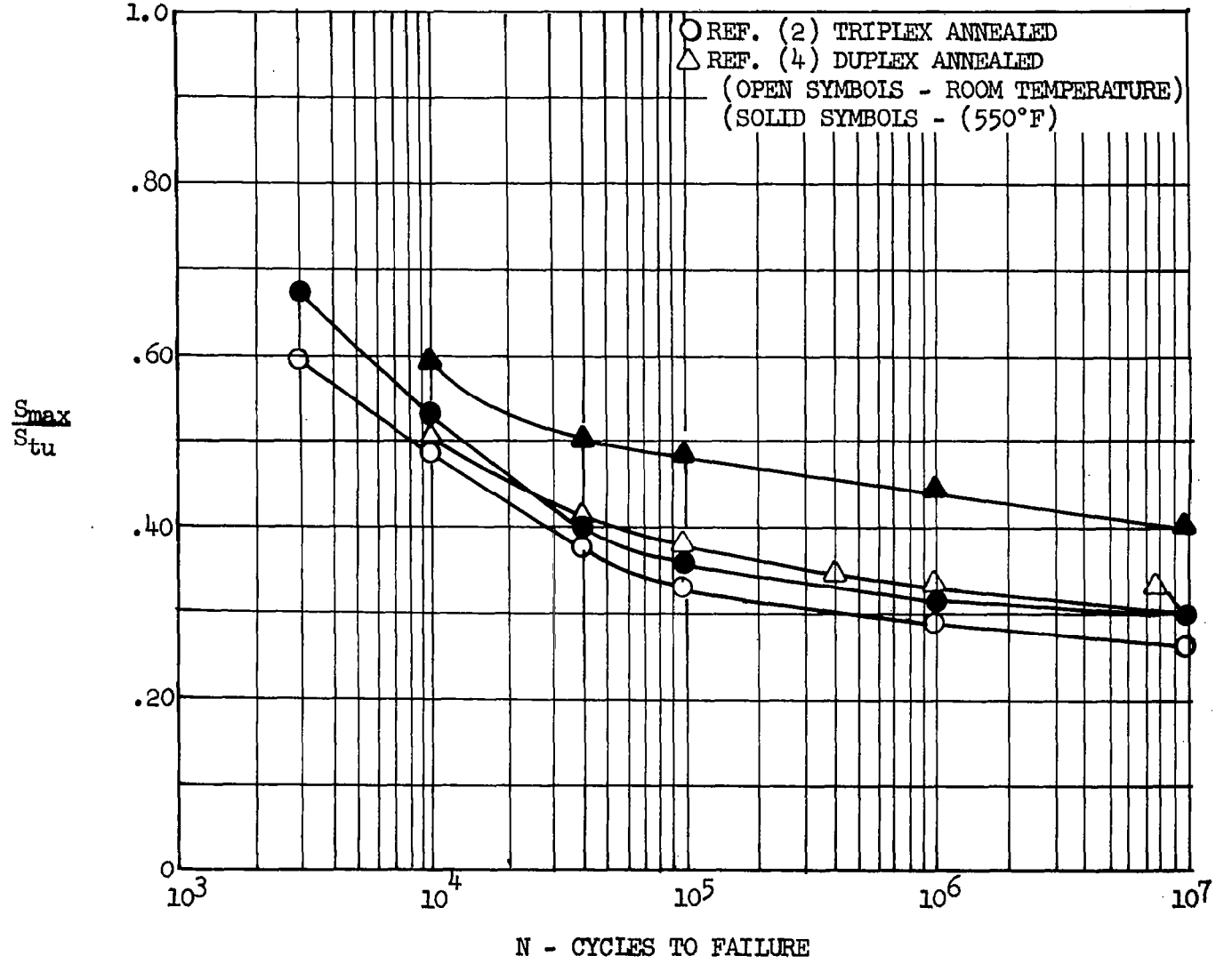

Figure 31. Comparison of Weld Metal Fatigue Life, K_t = 1.0, Smean = 25 ksi

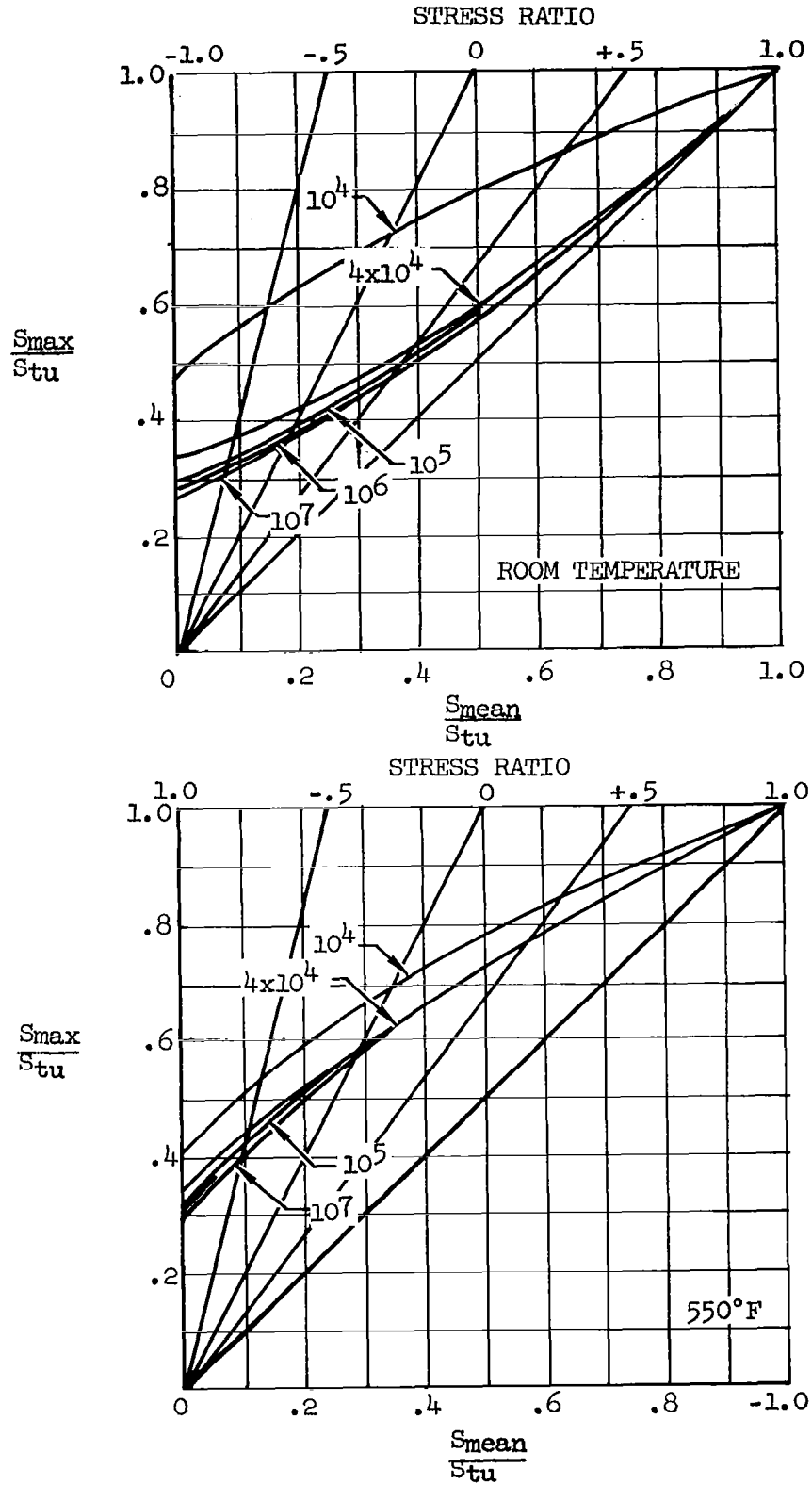

Figure 32. Estimated Fatigue Life Curves for Longitudinal Fusion Welds in Duplex Annealed Ti-8Al-1Mo-IV

"The aeronautical and space activities of the United States shall be conducted so as to contribute . . . to the expansion of human knowledge of phenomena in the atmosphere and space. The Administration shall provide for the widest practicable and appropriate dissemination of information concerning its activities and the results thereof."

—NATIONAL AERONAUTICS AND SPACE ACT OF 1958

NASA SCIENTIFIC AND TECHNICAL PUBLICATIONS

TECHNICAL REPORTS: Scientific and technical information considered important, complete, and a lasting contribution to existing knowledge.

TECHNICAL NOTES: Information less broad in scope but nevertheless of importance as a contribution to existing knowledge.

TECHNICAL MEMORANDUMS: Information receiving limited distribution because of preliminary data, security classification, or other reasons.

CONTRACTOR REPORTS: Scientific and technical information generated under a NASA contract or grant and considered an important contribution to existing knowledge.

TECHNICAL TRANSLATIONS: Information published in a foreign language considered to merit NASA distribution in English.

SPECIAL PUBLICATIONS: Information derived from or of value to NASA activities. Publications include conference proceedings, monographs, data compilations, handbooks, sourcebooks, and special bibliographies.

TECHNOLOGY UTILIZATION PUBLICATIONS: Information on technology used by NASA that may be of particular interest in commercial and other non-aerospace applications. Publications include Tech Briefs, Technology Utilization Reports and Notes, and Technology Surveys.

Details on the availability of these publications may be obtained from:

SCIENTIFIC AND TECHNICAL INFORMATION DIVISION

NATIONAL AERONAUTICS AND SPACE ADMINISTRATION

Washington, D.C. 20546